

# Fundamental tradeoffs in robust spectrum sensing for opportunistic frequency reuse

Anant Sahai

Niels Hoven

Shridhar Mubaraq Mishra

Rahul Tandra

sahai@eecs.berkeley.edu

nhoven@eecs.berkeley.edu

smm@eecs.berkeley.edu

tandra@eecs.berkeley.edu

Dept. of Electrical Engineering and Computer Science

University of California, Berkeley

## Abstract

Under the current system of spectrum allocation, spectral bands are allocated for time-scales ranging from years to decades and spatial scales ranging from counties to continents. Robust operation of devices is enabled by the use of guard bands in space and frequency. This paradigm has resulted in vastly underutilized spectrum bands, even in urban locales. However, advances in wireless technology now allow devices to operate on much smaller time and spatial scales. Like sand and pebbles poured into the gaps between larger rocks, such devices have the potential to greatly improve our overall spectrum utilization.

The fundamental constraint is robustly guaranteeing non-interference to privileged users of the band. We focus on cognitive radios that perform sensing and adapt their output to avoid interfering. We show that uncertainty in fading poses a serious challenge by forcing high sensitivity. These challenges are exacerbated by the presence of multiple users, but gains are available through cooperation. However, cooperative gains are limited by trust/reliability and the network's cooperation footprint. Furthermore, uncertainty regarding noise and interference imposes fundamental limits on how sensitive robust sensing can be. Local cooperation is necessary to provide fairness by reducing the uncertainty impact of other users' transmissions.

## I. INTRODUCTION

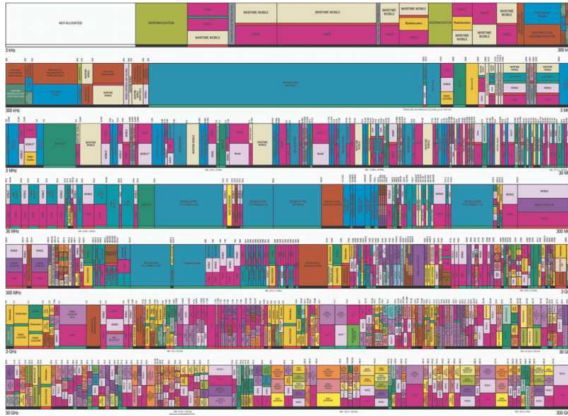
There is no doubt that the development and deployment of wireless technologies is one of the great achievements of the past century. Frequency division has allowed different systems to be deployed in a decoupled way, even when their spatial and temporal extents overlap. Since the filters used to isolate systems are not perfect and radio waves attenuate gradually with distance, static “guard bands” in both space and frequency are used to accommodate these imperfections and robustly prevent harmful interference. Both the structure of the guard bands and the frequency/space allocations themselves are determined by governmental regulatory agencies operating on a time-scale ranging from years to decades and with spatial-granularity that ranges from counties to continents. These allocation decisions are then enforced by the certification of equipment and the issuing of licenses for exclusive use.

Looking at the NTIA’s chart of these frequency allocations (Figure 1.a), it appears that we are in danger of running out of spectrum [1] since most bands have already been assigned to specific uses. However, allocation is only half the story since wireless links themselves operate on different, and often much smaller, space and time-scales. Figure 1.b,c show that much of the allocated spectrum is mostly underutilized [2]. This underutilization is typical [3], [4] and upon reflection, is a natural consequence of the distinct scales at which regulation and use occur — a vase filled with rocks still has plenty of room for sand.

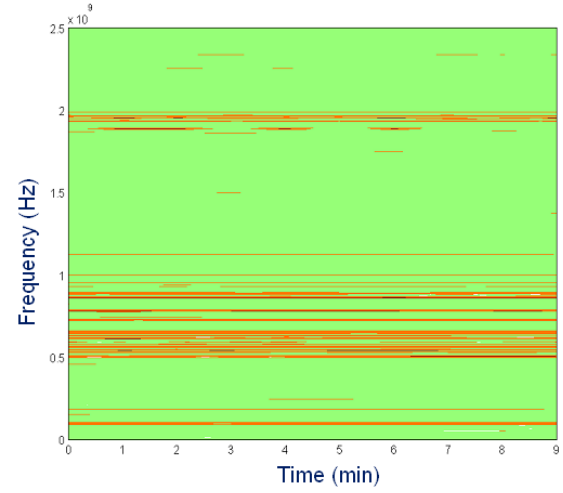
When the current regulatory model was adopted, radios were statically configured. Consequently, device certification was the only way to assure noninterference and robust operation. It was natural for allocations to operate on a timescale compatible with equipment lifespans and on a spatial extent compatible with device mobility and market size. As digital technology advanced, dynamic configuration became possible [6] and it became conceivable to exploit the vast spectral gaps that exist at the time and spatial scales of actual use.

### *A. The policy debate and alternatives*

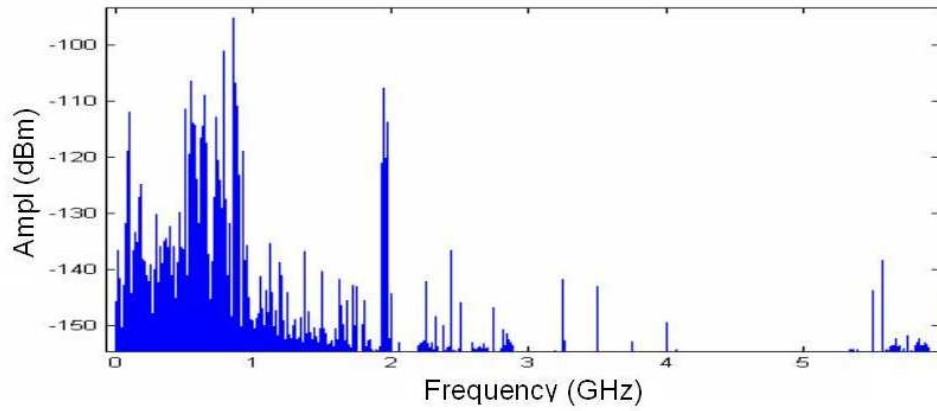
From an economic perspective, spectrum is an unimprovable finite, but infinitely renewable, resource that can be used as an input to provide useful services. The policy focus is therefore on putting it to the best possible use. The slow time-scale of the existing allocation process is recognized but is usually attributed to its centralized “command and control” nature with licensees having an exclusive right to do a specific thing only.



(a) The NTIA's spectrum allocation chart makes available spectrum look scarce.



(b) Usage varies with time



(c) Actual intensity of usage varies greatly by frequency.

Fig. 1. Measurements from the Berkeley Wireless Research Center show that there is great discrepancy between spectrum allocation and usage. Measurements were performed once every minute for a duration of  $1.6\mu\text{s}$  using a 20GHz ADC. The light background in (c) represents levels in the range of  $-130\text{dBm}$ . As a comparison, Dynamic Frequency Selection (DFS) techniques mandated for the 5.3GHz band need to switch frequencies when they detect received *power* levels in the range of  $-62\text{dBm}$  [5].

One proposed solution is simply eliminating legacy spectrum rights to a large extent and creating new comprehensive commons [7]. Commons proponents argue that the astonishing success of WiFi-style devices is proof that “unlicensed” devices can coexist in a largely unregulated way [8]. While usually discussed in terms of freedom and flexibility from red-tape, the commons approach is also implicitly a rejection of the separation of time-scales between allocation and actual use. Commons proponents assert that “wireless transmissions can be regulated by a combination of (a) baseline rules that allow users to coordinate their use, to avoid interference-producing collisions, and to prevent, for the most part, congestion, by conforming to equipment manufacturer’s specifications, and (b) industry and government-sponsored standards” [7]. However, there has been limited research into whether wildly heterogenous<sup>1</sup> wireless services can coexist using self-interested coordination. [9] reveals that in cases of severe asymmetry, self-interested behavior is not enough to guarantee either fairness or total utility whereas reasonably symmetric cases can in fact support a wide range of fair and efficient self-enforced equilibria.

Less radical solutions preserve a distinction between time-scales, spatial scales, as well as preserving a role for “primary users” given priority access to the spectrum. The common goal is increased productive utilization of the spectrum at the scale of actual use, but the exact rights afforded by this priority access depend on the approach chosen from Table I.

	Interference management primary’s responsibility	Interference management not primary’s responsibility
Secondary has permission	<b>Markets</b>	<b>Ultrawideband</b>
Secondary must take care	<b>Denials</b>	<b>Opportunistic</b>

TABLE I

THE FOUR APPROACHES TO FILLING SPECTRAL GAPS WHILE PRESERVING PRIORITY FOR PRIMARY USERS.

The “Markets” approach sits in the upper left corner of Table I and gives most of the power and responsibility to the primary user. To create the possibility for decentralized operations at a faster time-scale, this “flexible exclusive use model” proposes giving non-governmental parties

<sup>1</sup>Satellite or deep-space wireless services, cellular voice, and television broadcasts differ from each other by many orders of magnitude in power, range, etc.

responsibility for regulating the use of spectrum within a TAS package bounding time, area, and frequency ranges [10]. The interface between these regulatory zones is defined in terms of interference levels at service boundaries [11]. Responsibility for local regulation within a TAS package is expressed as a flexible property right with competition and profit motive providing the impetus to promoting the most effective uses [12]. The courts would enforce the privately determined allocation contracts. To effect the transition to a market, [13] recommends two-sided auctions where current licensees of spectrum can trade-in their spectrum for a combination of flexible rights and cash.

Flexibility to sub-license does not guarantee that any such sublicensing will actually take place. For that to happen, it must be profitable in the relevant secondary market. Efficiency also requires the prices to be informative in guiding use. An important approach is to conceptualize interference as congestion and consider pricing as a way to induce users to self-regulate their flows into the wireless network [14]. [15] presents an implementation of a market mechanism in which operators dynamically compete for spectrum and customers. However, collecting money from secondary users involves significant investment in infrastructure while market prices are likely to be very low in congestion-free locations with many gaps. Thus it seems unclear whether there is significant incentive to encourage the use of the spectrum that is currently wasted.

The upper-right approach in Table I is the ultrawideband (UWB) style that gives secondary users explicit permission to use the spectrum, but this permission is granted by the FCC, not the bands' primary users. To avoid interference to primary users, severe power limits are imposed and this limits UWB operation to short range links [16]. Furthermore, the wideband requirements prevent nearby UWB users from orthogonalizing themselves by frequency and thus UWB systems need to agree upon time-domain MAC protocols to avoid the severe penalties of non-orthogonal operation [9]. Of course, like any secondary use strategy, UWB performance will degrade as primary users start occupying their spectrum with higher power primary signals since these are interference from the perspective of the UWB receivers.

An alternative approach is to give secondary users only implicit permission to use the spectrum, allowing them to transmit only if they can do so without interfering with the primary system. The “denials” approach in the lower-left corner of Table I puts the burden of interference management on the primary. If secondaries are producing an unacceptable level of interference, the primary system issues a “shut up” order that must be obeyed. *But silence implies consent.* For one-to-

many radio systems like television, this requires retrofitting existing receivers to emit denial signals [17].

In the lower right corner of Table I, the interference management is the responsibility of secondary users who must seek out opportunities for noninterfering spectrum reuse. This is the regime for which cognitive radios have been proposed and has the advantage of internalizing all the costs to the agents that stand to gain without having to engage in external transactions. Cognitive radios dynamically adjust their transmissions in response to their environment [18] and are the focus of this paper.

### *B. Related Research*

Interest in cognitive radio approaches has recently increased tremendously. The proceedings of the first IEEE DySPAN conference in 2005 and the references therein provide useful background from the communication theory perspective. Although space limitations prevent us from giving a full survey here, there are two papers that are related to our work in spirit. [19] proposes a network of cognitive receivers near primary receivers in order to estimate the channel between the secondary transmitter and the primary receiver. In [20] a comprehensive method is proposed for detecting the presence of “white spaces” in spectrum usage that preferred stable gaps to more intermittent ones.

On the information theory side, [21] proposes a model of cognitive radio as a form of asymmetric cooperation. Rather than looking at operation within spectral gaps, they considered cognitive operation to be simultaneous with a strong primary signal. They define a generalized cognitive radio channel as an  $n$ -transmitter,  $m$ -receiver interference channel in which sender  $i$  obtains (causally or non-causally) the messages of senders 1 through  $i - 1$ . The rate region was extended to cognitive multiple access networks in [22].

### C. Overview

Many of the fundamental new issues are common to the different approaches to spectrum sharing from Table I. With the exception of ultrawideband, the approaches all require frequency-agile radios that are able to dynamically reconfigure themselves in response to their local situation to avoid causing interference. The essential power-control issues are common to all three. All of them must guarantee very robust operation for the primary in the face of uncertainties coming from the environment, hardware, other users, etc. The traditional role played by static space and frequency guard bands in guaranteeing robustness must be played by dynamic algorithms and protocols. As a result, all of these approaches pose a challenge to the existing paradigm of regulation by static certification of devices.

After first discussing the common signal processing roots of the fundamental limits in Section II, we focus on the case of opportunistic use in which the secondaries must use their own sensing capabilities to avoid trampling vulnerable primary receivers. We believe that similar issues will also manifest themselves in the case of secondary market<sup>2</sup> and explicit denial<sup>3</sup> based approaches. A core challenge to a purely local sensing based approach arises due to uncertainties in fading.

Some of the most promising bands for unlicensed devices are the TV broadcast bands. The FCC has already released a Notice Of Proposed Rule Making exploring the operation of unlicensed devices on spatially/temporally “unused” television broadcast bands [23]. The case of geographically sparse, powerful users has the most potential for secondary devices to be squeezed into the interstices between primary systems. Showing that significant cooperation is necessary in the TV bands indicates that even greater cooperation will be necessary to protect primary systems with smaller footprints.

We begin with a motivating example to illustrate the necessity of detecting undecodable signals. A naive designer might build a cognitive radio that falls silent if it can decode the primary system’s transmission and talks otherwise. We will show that this rule is inadequate.

<sup>2</sup>In particular, detecting and proving infringement will be a challenge in the face of these types of uncertainties.

<sup>3</sup>The problem of robustly detecting primaries maps to the similar problem of robustly detecting denial signals as well as the problem of distinguishing signals degraded due to harmful interference from those that would be hopelessly attenuated even without the interference from secondaries.

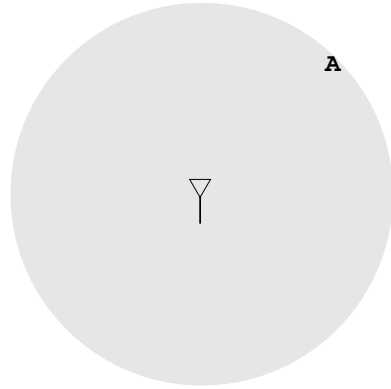
For simplicity, we begin by considering the case of a single cognitive radio transmitter with a known maximum transmit power.

1) *Protecting privileged users:* In our model, we assume a band already potentially assigned to a high-powered single-transmitter system (television, for example). All transmissions are assumed to be omnidirectional. Figure 2a depicts a transmitter from the primary system. The dotted circle represents the boundary of decodability for a single-transmitter system. That is, in the absence of all interference, a user within the dotted line would be able to decode a signal from the transmitter, while a user outside the circle would not. Our goal when introducing a cognitive radio system is to maintain a guarantee of service to legacy users. We can control the interference experienced by a primary receiver by declaring a “no-talk” zone around it, within which the secondary transmitter is constrained to be silent. (This idea is examined in detail in Section III)

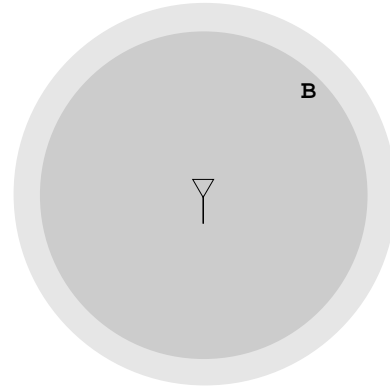
However, if we want to actually create a system in which we guarantee performance to every primary user within the decodability circle, we run into a problem. Primary users (depicted with capital letters in the figures) on the very edge of the decodability region will suffer under any change to the exclusive-use model. Consider receiver A, located on the border of the decodability region (Figure 2a). Any amount of interference, no matter how infinitesimal, will cause A to lose its ability to decode. Its no-talk zone must include the entire world!

Therefore, it is clear that we must build some sort of buffer into our protected radius. Let the shaded circle represent the “protected region” where we guarantee decodability to primary receivers. Within this protected radius, all unshaded primary receivers must be guaranteed reception, even when the cognitive radios are operating. The more we shrink the bound of the protected region inside the decodability region, the smaller the necessary no-talk zones become. Conversely, we cannot protect everybody. As the protected radius approaches the limit of decodability, the no-talk zones grow dramatically (Figure 2b). The size of the no-talk zones also depend on the cognitive radio’s maximum transmit power (Figure 3a).

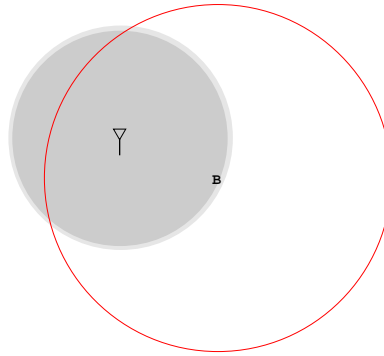
Many proposed uses for cognitive radios focus on the utility of large networks of cheap, low-powered devices. We consider the case of a purely local-sensing based approach. If a cognitive radio cannot tell where the primary system’s receivers are located, secondary users must stay out of the area that is the union of all possible no-talk zones (4a). Even if the individual no-talk zones are small, this uncertainty in the primary receivers’ locations can result in a large global no-talk zone. We note that in the hypothetical example, the prohibited region for the secondary



(a) The light circle represents the decodability radius, the maximum distance at which the transmitted signal can be decoded assuming only propagation path loss.

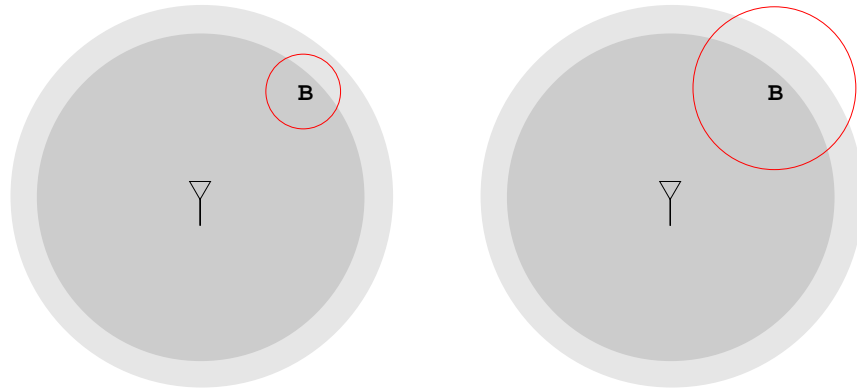


(b) The darker circle represents the protected radius. Users inside the protected radius must be guaranteed service with only a low  $P_{HI}$  probability of excessive harmful interference.



(c) As the protected radius approaches the limit of decodability, the no-talk zones grow dramatically.

Fig. 2. We assume a single high-powered primary transmitter, for example, television [23]. The highest priority constraint for opportunistic devices is maintaining a guarantee of non-interference to the official user of the spectrum (primary system). This is done by enforcing no-talk zones around primary receivers. We cannot extend this guarantee to everyone (user A, on the border of the decodability radius would lose service with an infinitesimal amount of interference) so we declare a “protected region” inside the decodable radius.

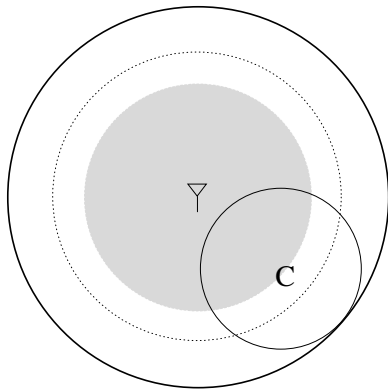


(a) If the secondary user is a “mouse”, who squeaks softly with low power transmissions, then the no-talk zones around each receiver can be much smaller.

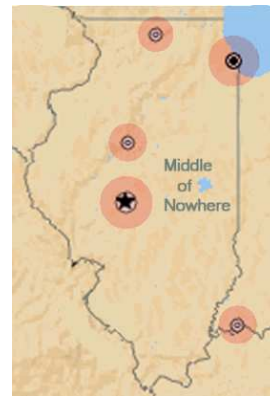
(b) If the secondary user is a “lion”, roaring with high power transmissions, the radii of the no-talk zones will become much larger.

Fig. 3. Our goal when introducing a cognitive radio system is to maintain a guarantee of service to legacy users. We can control the interference experienced by a primary receiver by declaring a “no-talk” zone around it, within which the secondary transmitter is constrained to be silent.

user has already extended beyond the decodability region.



(a) We protect all possible receiver locations

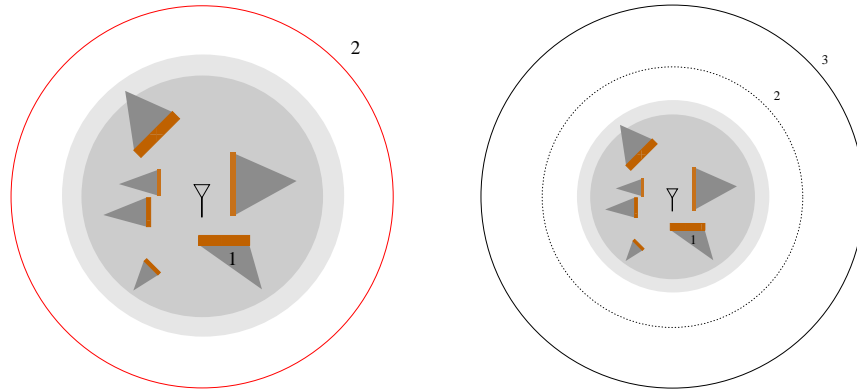


(b) Still plenty of reclaimable space

Fig. 4. If we don’t know exactly where the primary receivers are, we must protect everywhere they might possibly be. We can still reclaim plenty of spectrum in the middle of nowhere.

Though it may at first seem problematic that the required quiet zones are so large, we remind

the reader that our goal was to increase the spectrum available to users in the middle of nowhere. These users are still well outside the quiet zones (4b).



(a) If a secondary user detects a low SNR signal, it has no way to tell if it is well outside the protected region (user 2), or in the global quiet zone but behind a building (user 1). An identical problem occurs as a result of multipath fading.

(b) A secondary user might be faded while his transmissions could still reach an unfaded primary receiver. A secondary user who can not distinguish between positions must be quiet in both. Secondary users must now detect very weak signals to be sure they are outside the original no-talk zone (user 3).

Fig. 5. If we take shadowing/fading with respect to the primary transmitter into account, the prohibited region grows. A secondary transmitter who cannot tell if he is in a shadow must hear a much weaker signal to be certain he will not interfere.

2) *Shadowing effects:* If we take shadowing with respect to the primary transmitter into account (Figure 5), the prohibited region continues to grow. If a secondary user (depicted with lowercase letters in the figures) detects a low SNR signal (Figure 5b), it has no way to tell if it is well outside the protected region (user a), or in the global quiet zone but behind a building (user b). To avoid locally shadowed secondary users interfering with unshadowed primary users (user C), the no-talk zone must be pushed out even further. The outermost circle represents the quiet zone such that the maximum SNR on its border equals the minimum SNR within the unshadowed case's protected region. We can mitigate this effect through cooperation (Figure 6).

Figure 7 summarizes the main drawbacks of a local-sensing based approach.

3) *Interference suppression through decodability:* As mentioned before, the intuitive rule for interference control is requiring secondary transmitters to fall silent if they can decode the

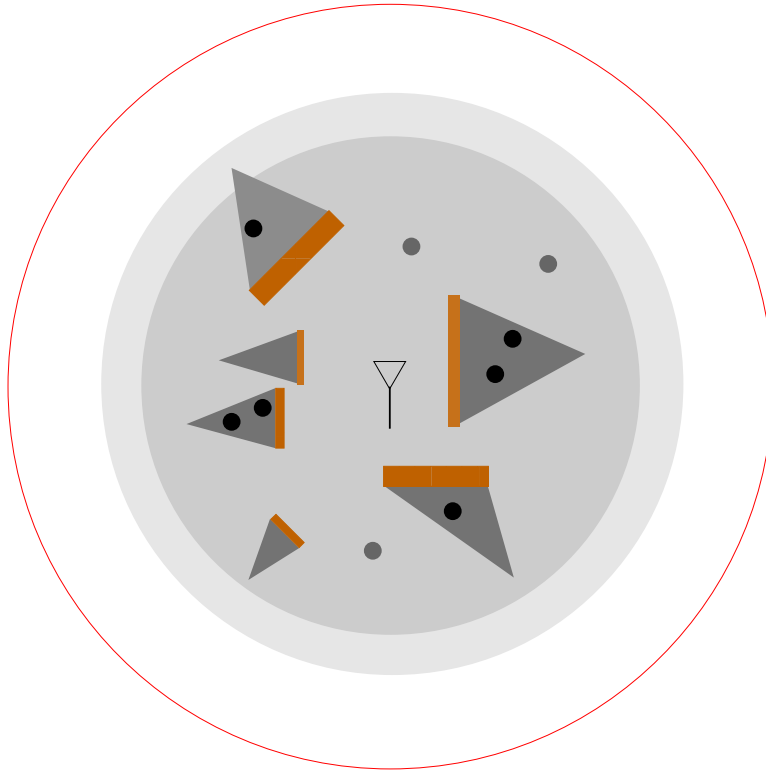


Fig. 6. Cooperation within a geographically distributed network of secondary users avoids dealing with the worst-cases of fading. Secondary users should detect the primary collectively!

primary’s signal and allowing them to transmit if they cannot. A first principles analysis has already indicated the necessity of placing the border of the no-talk zone outside the decodability radius. However, let us examine the repercussions of insisting on using the “don’t transmit if you can decode” rule.

We make the optimistic assumption that primary and secondary users experience the same propagation-related path loss. This means that no unshadowed cognitive radios will be transmitting inside the decodability region. For practical systems, such as if the primary receiver is a finely tuned television aerial on top of a house, and the secondary user is a cheap mobile unit on the ground, this may not be the case. We also assume the secondary user may be additionally shadowed up to 10 dB with respect to the primary transmitter.

For illustrative purposes, we assume a broadcast TV transmitter with a decodability radius 52 km away. We also assume the signal decays as  $r^{-3.5}$ . In Section III, we show that in an ideal

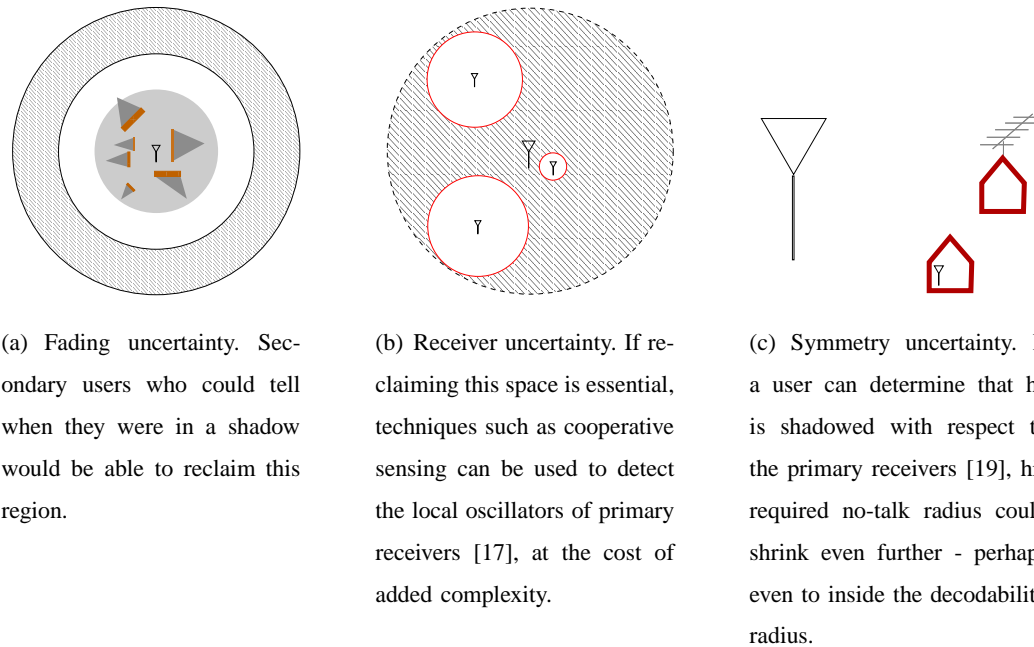


Fig. 7. If a secondary user must detect a 10 dB shadow with respect to the primary transmitter (we assume attenuation as  $r^{-3.5}$  and the decodability limit at the Grade B contour for a TV transmitter), the effective no-talk zone is pushed out by 10 dB, from 52 km to 100 km. This area measures  $\pi 100^2 - \pi 52^2 \approx 23,000 \text{ km}^2$ . The worst case penalty for receiver uncertainty occurs when there are no primary receivers at all, but the secondary users are forced to respect the protected area anyway. In this case, knowing where primary receivers are (or aren't) opens up the entire protected region for secondary usage, reclaiming  $\pi 52^2 \approx 8400 \text{ km}^2$  of land which would otherwise be underutilized. In this example, overcoming mild shadowing reclaims nearly 3 times as much area as does knowing the primary receivers' locations.

world, free of shadowing and fading, the “don't transmit if you can decode” rule is actually feasible. However, the rule's usefulness is drastically curbed by shadowing.

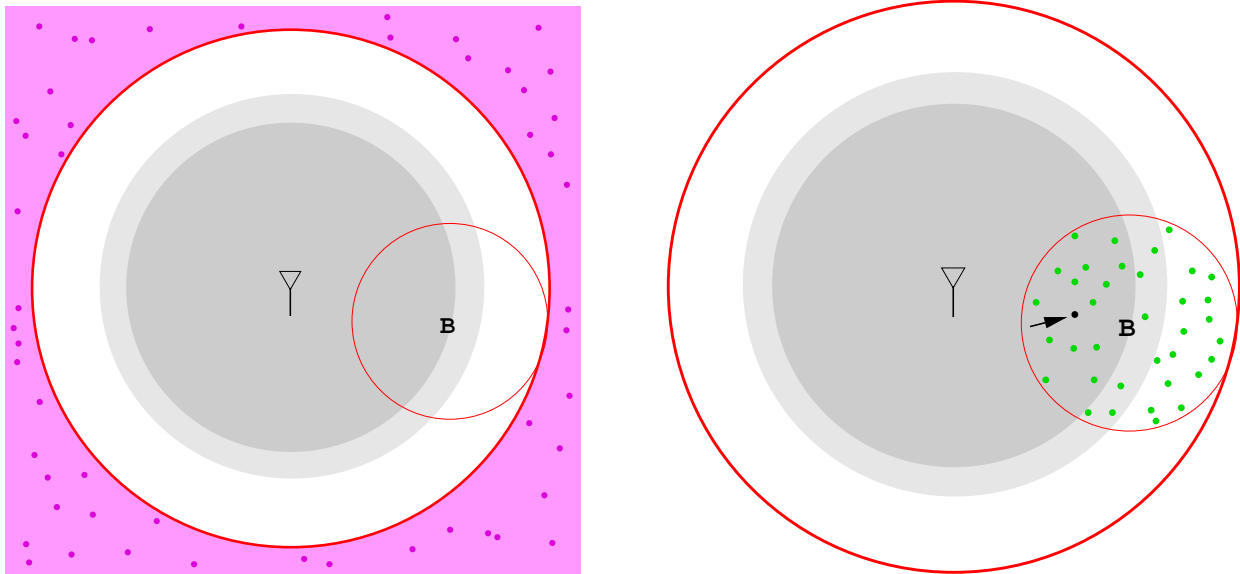
If cognitive radios are allowed to begin talking when they can no longer decode the signal, the possibility of 10 dB of shadowing puts the edge of the no-talk zone 10 dB inside the decodability radius. Since a secondary user cannot be allowed to transmit right next to a primary user, this leaves us with two options. Either we give up and do not allow secondary users to transmit at all, or we stick with the proposed rule and simply shrink the protected radius. If secondary users begin transmitting 10 dB inside the protected radius, the protected radius must end at least 10 dB inside the protected radius. (It must actually be somewhat more, in order to allow for some attenuation of the secondary transmissions.)

This may not seem like a big deal. After all, the TV signal is attenuated by 165 dB between

the transmitter and the decodability radius, so shrinking the protected radius by 10 dB doesn't at first appear to be a huge sacrifice. However, allowing this 10 dB margin shrinks the protected radius from 52 km to just 27 km. After implementing this misguided rule, we can only protect users in 27% of the original service area! The only alternative is to ban secondary users entirely. It should be clear that the "don't transmit if you can decode a signal" rule is woefully inadequate.

4) *Multiple users*: The presence of multiple users presents new challenges, but also new opportunities for cooperation. Section III discusses the resulting tradeoff between secondary power density and required sensing, taking into account the multiuser issues illustrated in Figure 8.

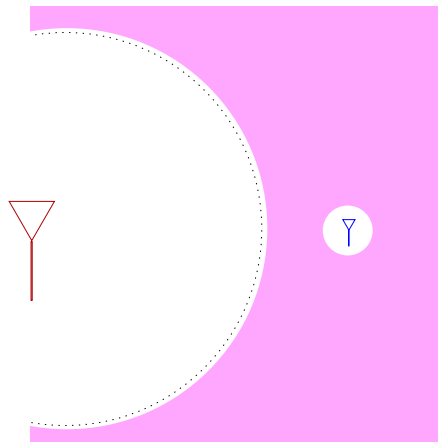
Section IV shows how cooperation with moderately distant secondary users (illustrated in Figure 6) is required to overcome fading uncertainty, and that the cooperative gains are fundamentally limited by uncertainties related to trust as well as the effective cooperation footprint of the cognitive network. Finally, Section V shows that local cooperation (illustrated in Figure 9) is required to provide fairness and to overcome the uncertainty coming from the unknown distribution of active secondary users.



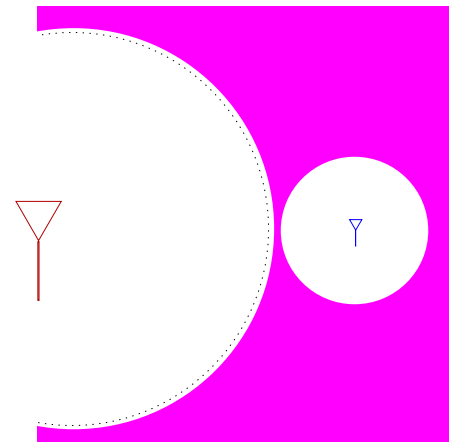
(a) Outside the no-talk zone, we are primarily concerned with the aggregate interference. One cognitive radio may not cause excessive interference to a primary receiver, but what there are millions of secondary transmitters?

(b) Inside the no-talk zone, we must accept that no detector is perfect. Secondary users will occasionally miss detection of the primary signal, and transmit, thereby interfering with nearby primary systems. With only one cognitive radio present, a rare mistake is not a serious problem. However, if there are many cognitive radios present, their detectors must be far more accurate.

Fig. 8. The presence of multiple cognitive radios presents new challenges.



(a) Low density requires less coordination



(b) High density, high coordination

Fig. 9. If a secondary system cannot robustly distinguish between the transmissions of the primary system and those of other secondary systems, it will fail to capitalize on situations where the spectrum is available but is already being used by another secondary system farther away. The presence/absence of possible interference from other opportunistic spectrum users represents a major component of the uncertainties limiting the ability of a sensor network to reclaim a band for its use. As a solution, we propose the existence of a mandated “sensing MAC” among systems which ensures that whenever a particular sensor node is sensing for the primary signal, all sensors within a certain “shut-up” radius refrain from transmitting. Increased density of secondary transmissions requires greater cooperation.

## II. LIMITS TO ROBUST SIGNAL PROCESSING

In this section we consider the problem of detecting the presence or absence of a low SNR signal in the ‘band of interest’ (see Figure 10). For simplicity, we initially model the primary signal  $X(t)$  as white and corrupted by white noise  $W(t)$ . By sampling the band of interest at the Nyquist rate, this is formulated as a binary hypothesis testing problem, where the aim is to distinguish the following hypotheses:

$$\begin{aligned}\mathcal{H}_0 : Y[n] &= W[n] & n = 1, \dots, N \\ \mathcal{H}_1 : Y[n] &= X[n] + W[n] & n = 1, \dots, N\end{aligned}\quad (1)$$

Where  $X[n]$  are i.i.d signal samples and  $W[n]$  are i.i.d noise. We are interested in decision strategies that robustly achieve a given target probability of false alarm,  $P_{FA}$ , and probability of missed detection,  $P_{MD}$ .

### Spectrum picture

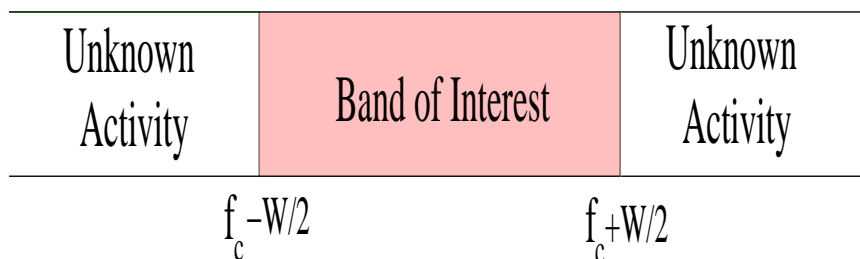


Fig. 10. Big question: sensing the primary

The sample complexity of a detector captures how the dwell time  $N$  varies with  $SNR$  for given  $P_{FA}$  and  $P_{MD}$ <sup>4</sup>. It has been shown in [24], [25] that the sample complexity for energy detection or a radiometer is  $O(SNR^{-2})$ , [26]. However, if the primary signal had a deterministic part then matched filtering would attain a sample complexity of  $O(SNR^{-1})$  [27]. We now derive the sample complexity of the optimal detector in the case when the signal is zero-mean and has low power.

<sup>4</sup>Good sample complexity performance is important because the dwell time is a key resource for cognitive radio systems

### A. Sample Complexity of detection: non-coherent detector

We begin with the following notation: The signal to noise ratio is denoted by  $SNR$  in this paper. When we express the signal to noise ratio in dB (in most of our figures), we explicitly mention it. Also, for most part of the paper, we assume that the  $SNR$  is the average signal to noise ratio. When we work with the peak signal to noise ratio, we explicitly mention it beforehand.

In this section we assume that the signal samples  $X[n]$  are i.i.d random variables having finite support, i.e.,  $X[n]$  takes values from a finite set  $\{x_1, x_2, \dots, x_M\}$  with  $Pr(X[n] = x_i) = p_i$ . Furthermore, we assume that the signal constellation is zero-mean, i.e.,  $\sum_{i=1}^M p_i x_i = 0$  and the signal amplitude is significantly lower than the noise power, i.e.,  $|x_i|^2 \ll \sigma^2$ . This automatically implies that the average signal power,  $P := \sum_{i=1}^M p_i x_i^2$  satisfies,  $P \ll \sigma^2$ .

We now derive the log-likelihood ratio in the Neymen-Pearson test for the detection problem in (1).

$$\begin{aligned}
LLR(\mathbf{Y}) &= \sum_{n=1}^N \log \left[ \frac{Pr(Y[n]|\mathcal{H}_1)}{Pr(Y[n]|\mathcal{H}_0)} \right] \\
&= \sum_{n=1}^N \log \left[ \frac{\left[ \sum_{i=1}^M p_i Pr(Y[n]|\mathcal{H}_1, X[n] = x_i) \right]}{Pr(Y[n]|\mathcal{H}_0)} \right] \\
&= \sum_{n=1}^N \log \left[ \frac{\left[ \sum_{i=1}^M p_i \left( \frac{1}{\sqrt{2\pi\sigma^2}} \exp -\frac{(Y[n]-x_i)^2}{2\sigma^2} \right) \right]}{\left( \frac{1}{\sqrt{2\pi\sigma^2}} \exp -\frac{Y[n]^2}{2\sigma^2} \right)} \right] \\
&= \sum_{n=1}^N \log \left[ \sum_{i=1}^M p_i \exp -\frac{x_i^2}{2\sigma^2} \exp \frac{x_i Y[n]}{\sigma^2} \right] \\
&:= \sum_{n=1}^N f \left( \frac{Y[n]}{\sigma^2} \right) \tag{2}
\end{aligned}$$

where we use the function  $f(t) := \log \left[ \sum_{i=1}^M p_i \exp -\frac{x_i^2}{2\sigma^2} \exp x_i t \right]$  to simplify the notation. From (2) we note that the log-likelihood ratio is a sum of  $N$  i.i.d. random variables under each hypothesis. Since the dwell time  $N$  is typically large for low SNR detection, we can use the Central Limit Theorem, to approximate the  $LLR$  as a Gaussian random variable. Also, note that the optimal decision strategy is to decide based on the following rule:

$$LLR(\mathbf{Y}) \underset{\mathcal{H}_0}{\overset{\mathcal{H}_1}{\gtrless}} \gamma \tag{3}$$

for some threshold  $\gamma$ .

1) *Error probability analysis:* The probability of false alarm,  $P_{FA}$ , is given by:

$$\begin{aligned}
P_{FA} &= Pr(LLR(\mathbf{Y}) > \gamma | \mathcal{H}_0) \\
&= Pr\left(\sum_{i=1}^N f\left(\frac{Y[n]}{\sigma^2}\right) > \gamma | \mathcal{H}_0\right) \\
&= Pr\left(\frac{\sum_{i=1}^N f\left(\frac{Y[n]}{\sigma^2}\right) - N\mathbb{E}\left[f\left(\frac{Y[n]}{\sigma^2}\right)\right]}{\sqrt{NVar\left(f\left(\frac{Y[n]}{\sigma^2}\right)\right)}} > \frac{\gamma - N\mathbb{E}\left[f\left(\frac{Y[n]}{\sigma^2}\right)\right]}{\sqrt{NVar\left(f\left(\frac{Y[n]}{\sigma^2}\right)\right)}} | \mathcal{H}_0\right) \\
&= \mathcal{Q}\left(\frac{\gamma - N\mathbb{E}\left[f\left(\frac{Y[n]}{\sigma^2}\right) | \mathcal{H}_0\right]}{\sqrt{NVar\left(f\left(\frac{Y[n]}{\sigma^2}\right) | \mathcal{H}_0\right)}}\right)
\end{aligned} \tag{4}$$

Here we have used the Central Limit Theorem to justify  $\frac{\sum_{i=1}^N f\left(\frac{Y[n]}{\sigma^2}\right) - N\mathbb{E}\left[f\left(\frac{Y[n]}{\sigma^2}\right)\right]}{\sqrt{NVar\left(f\left(\frac{Y[n]}{\sigma^2}\right)\right)}} \sim \mathcal{N}(0, 1)$ .

Similarly, the probability of detection,  $P_D$ , is given by

$$\begin{aligned}
P_D &= Pr(LLR(\mathbf{Y}) > \gamma | \mathcal{H}_1) \\
&= \mathcal{Q}\left(\frac{\gamma - N\mathbb{E}\left[f\left(\frac{Y[n]}{\sigma^2}\right) | \mathcal{H}_1\right]}{\sqrt{NVar\left(f\left(\frac{Y[n]}{\sigma^2}\right) | \mathcal{H}_1\right)}}\right)
\end{aligned} \tag{5}$$

For convenience we use the following notation:

$$\begin{aligned}
m_0 &:= \mathbb{E}\left[f\left(\frac{Y[n]}{\sigma^2}\right) | \mathcal{H}_0\right] \\
m_1 &:= \mathbb{E}\left[f\left(\frac{Y[n]}{\sigma^2}\right) | \mathcal{H}_1\right] \\
\sigma_0^2 &:= Var\left(f\left(\frac{Y[n]}{\sigma^2}\right) | \mathcal{H}_0\right) \\
\sigma_1^2 &:= Var\left(f\left(\frac{Y[n]}{\sigma^2}\right) | \mathcal{H}_1\right)
\end{aligned}$$

Eliminating the threshold,  $\gamma$  from (4) and (5) we obtain the sample complexity to be

$$N = \left[\frac{\mathcal{Q}^{-1}(P_{FA})\sigma_0 - \mathcal{Q}^{-1}(P_D)\sigma_1}{(m_1 - m_0)}\right]^2 \tag{6}$$

In order to see the behavior of  $N$  as a function of  $SNR$  in (6) we need to evaluate  $m_0$ ,  $m_1$ ,  $\sigma_0$  and  $\sigma_1$  as a function of  $SNR$ . However, it is not possible to get a closed form expression for the above mentioned quantities. Hence, we try to approximate and get the essential order of magnitude behavior.

To do so, we first expand  $f\left(\frac{Y[n]}{\sigma^2}\right)$  using the Taylor series at 0 to get

$$f\left(\frac{Y[n]}{\sigma^2}\right) = f(0) + \frac{f'(0)}{1} \left(\frac{Y[n]}{\sigma^2}\right) + \frac{f''(0)}{2} \left(\frac{Y[n]}{\sigma^2}\right)^2 + \text{higher order terms}$$

Since  $\frac{Y[n]}{\sigma^2} \ll 1$  under both hypotheses, we can approximate  $f\left(\frac{Y[n]}{\sigma^2}\right)$  by ignoring the higher order terms in the Taylor series expansion. Actually computing the first and the second derivative of  $f(t)$  at  $t = 0$ , we get

$$\begin{aligned} f'(0) &= \frac{\sum_{i=1}^M x_i p_i \exp\left(-\frac{x_i^2}{2\sigma^2}\right)}{\sum_{i=1}^M p_i \exp\left(-\frac{x_i^2}{2\sigma^2}\right)} \\ f''(0) &= \frac{\sum_{i=1}^M x_i^2 p_i \exp\left(-\frac{x_i^2}{2\sigma^2}\right)}{\sum_{i=1}^M p_i \exp\left(-\frac{x_i^2}{2\sigma^2}\right)} - [f'(0)]^2 \end{aligned}$$

Since, we have assumed that  $|x_i|^2 \ll \sigma^2$ , we can assume that  $\exp\left(-\frac{x_i^2}{2\sigma^2}\right) \approx 1$ . Hence, we have

$$\begin{aligned} f'(0) &\approx \frac{\sum_{i=1}^M x_i p_i}{\sum_{i=1}^M p_i} \\ &= 0 \quad \left( \text{Since } \sum_{i=1}^M x_i p_i = 0 \right) \\ \Rightarrow f''(0) &\approx \frac{\sum_{i=1}^M x_i^2 p_i}{\sum_{i=1}^M p_i} \\ &= P \end{aligned}$$

Therefore, neglecting the higher order terms in the Taylor series expansion of  $f(t)$  and using the above approximations we get

$$\begin{aligned} f\left(\frac{Y[n]}{\sigma^2}\right) &\approx f(0) + \frac{P Y[n]^2}{2 \sigma^4} \\ &= f(0) + \frac{SNR Y[n]^2}{2 \sigma^2} \end{aligned}$$

Using the above approximation we have

$$m_0 = f(0) + \frac{SNR}{2} \left( \frac{\mathbb{E}(Y^2[n]|\mathcal{H}_0)}{\sigma^2} \right)$$

Similarly, we have

$$m_1 = f(0) + \frac{SNR}{2} \left( \frac{\mathbb{E}(Y^2[n]|\mathcal{H}_1)}{\sigma^2} \right)$$

Hence,

$$\begin{aligned} m_1 - m_0 &= \frac{SNR}{2\sigma^2} [\mathbb{E}(Y[n]^2|\mathcal{H}_1) - \mathbb{E}(Y[n]^2|\mathcal{H}_0)] \\ &= \frac{SNR}{2\sigma^2} [(P + \sigma^2) - \sigma^2] \\ &= \frac{SNR^2}{2} \end{aligned}$$

Similar calculations for the variances give

$$\begin{aligned} \sigma_0^2 &= \frac{SNR^2}{2} \\ \sigma_1^2 &= \frac{SNR^2}{2} (2SNR + 1) \\ &\approx \frac{SNR^2}{2} \end{aligned}$$

Substituting these in (6) we get

$$\begin{aligned} N &= \left[ \frac{\frac{SNR}{\sqrt{2}} (\mathcal{Q}^{-1}(P_{FA}) - \mathcal{Q}^{-1}(P_D))}{\frac{SNR^2}{2}} \right]^2 \\ &= 2[\mathcal{Q}^{-1}(P_{FA}) - \mathcal{Q}^{-1}(P_D)]^2 SNR^{-2} \end{aligned} \quad (7)$$

Hence, we have just proved the following theorem.

**Theorem 1:** Consider the problem of detecting the presence or absence of a zero-mean signal in the presence of additive Gaussian noise (eqn. (1)). For this problem, the sample complexity of detection for the optimal detector is given by,

$$N \approx 2[\mathcal{Q}^{-1}(P_{FA}) - \mathcal{Q}^{-1}(P_D)]^2 SNR^{-2}$$

This shows that the optimal detector performs as badly as the radiometer.

Figure 11 shows that sample complexity of detection when the signal samples are drawn from a BPSK constellation. It can be clearly seen that the energy detector performs just as well as the optimal detector. However, the presence of a pilot tone improves the sample complexity drastically.

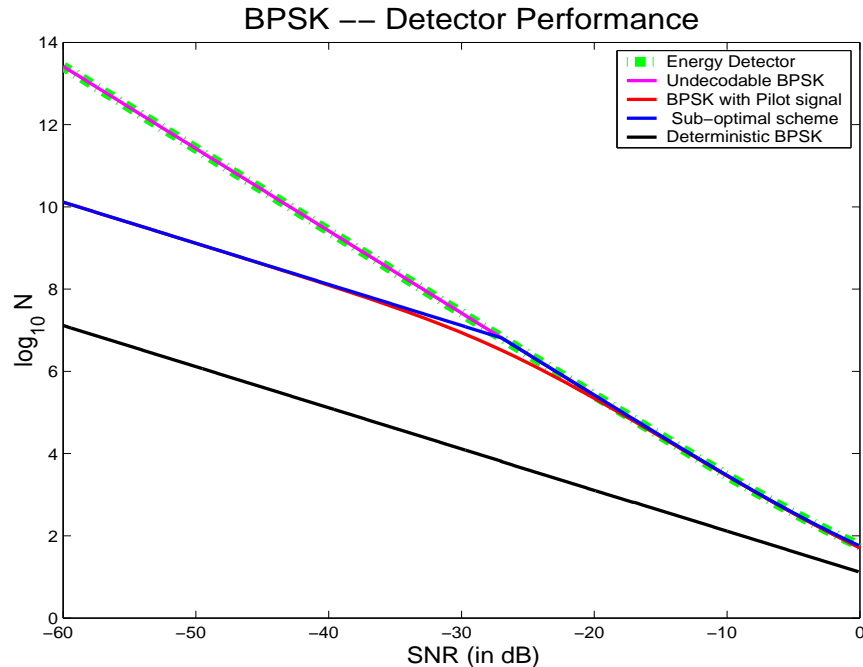


Fig. 11. The figure compares the sample complexity curves for an undecodable BPSK signal without a pilot and the sample complexity curves of an undecodable BPSK signal with a known pilot signal. The order of the curves follows the legend. The dashed green curve shows the performance of the energy detector, the pink curve corresponds to the performance of the optimal detector. Both these curves are for the case without a pilot signal. These curves show that the energy detector performance is same as that of the optimal detector. The red curve gives the performance of the optimal detector in the presence of a known weak pilot signal. Note, that there is a significant decrease in sample complexity due to the known pilot signal, especially at very low SNR. Specifically, at low SNR, the sample complexity changes from  $O(1/SNR^2)$  to  $O(1/SNR)$  due the presence of the pilot.

### B. Detector robustness: non-coherent case

In any practical system, the random distributions are never known perfectly. From a signal processing perspective, the main source of uncertainty in a cognitive radio system is the noise at the receiver. Noise is an aggregation of various sources like thermal noise, leakage of signals from other bands due to receiver non-linearities, aliasing from imperfect front end filters, interference due to transmissions from other users far away, interference from other opportunistic systems in the vicinity, etc. Assuming that these noise statistics are completely known is not reasonable. A Gaussian assumption is only an approximation and it is reasonable to assume that there is always some *residual uncertainty* in our noise estimate, even after run-time calibration.

In traditional communication, the focus is on demodulating and decoding the signal. Once

we are looking in the relevant degrees of freedom, the noise is usually smaller than the desired signal since there is little interest in acquiring signals that will be undecodable. As a result, it is usually safe to ignore this noise uncertainty or to just overbound it with a worst case Gaussian.

For detection, the story is different since we do not need to demodulate or decode. For simplicity we start by discussing the robustness of a radiometer under noise level uncertainty [28]. Since the radiometer only sees energy, the distributional uncertainty can be summarized in a single interval  $[\sigma_{low}^2, \sigma_{high}^2]$  where  $\sigma^2$  is the noise power. As illustrated in Figure 12, it is clear that the radiometer will not be able to robustly detect the signal if the signal strength is less than the threshold  $(\sigma_{high}^2 - \sigma_{low}^2)$ . The presence of the signal is indistinguishable from a larger value for the noise. Figure 13 plots the *SNR* threshold for the radiometer as a function of the noise uncertainty.

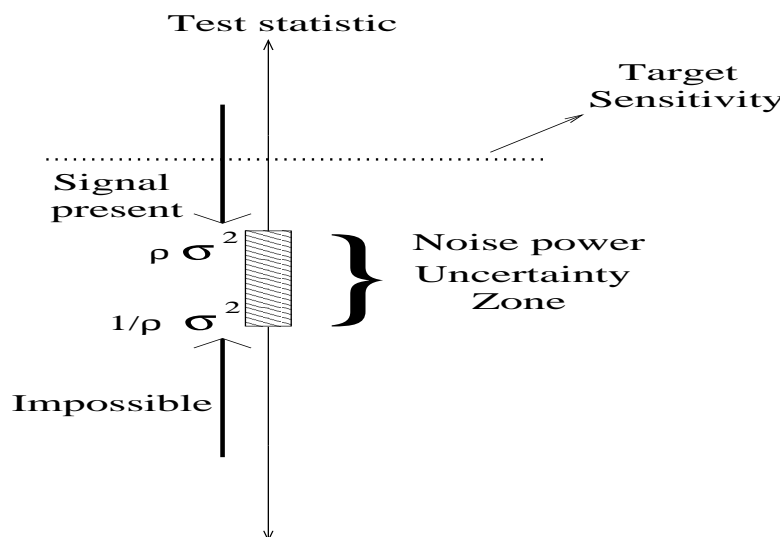


Fig. 12. Understanding device level noise uncertainty in the case of a radiometer. The shaded area in the figure represents the uncertainty in the noise power. It is clear from the figure that if the test statistic falls within the shaded region, there is no way to distinguish between the two hypotheses. Hence the radiometer hits an SNR wall, and is non-robust to simple device level uncertainties.

We now consider the robustness of any general detector under noise uncertainty parametrized by a number, say  $x$  dB. The unknown noise comes from a class of distributions that includes a set  $\mathcal{W}_x$  with  $W_a \in \mathcal{W}_x$  satisfying the following properties:

- The noise process is ‘white’ and symmetric,  $\mathbb{E}W_a^{2k-1} = 0$ .

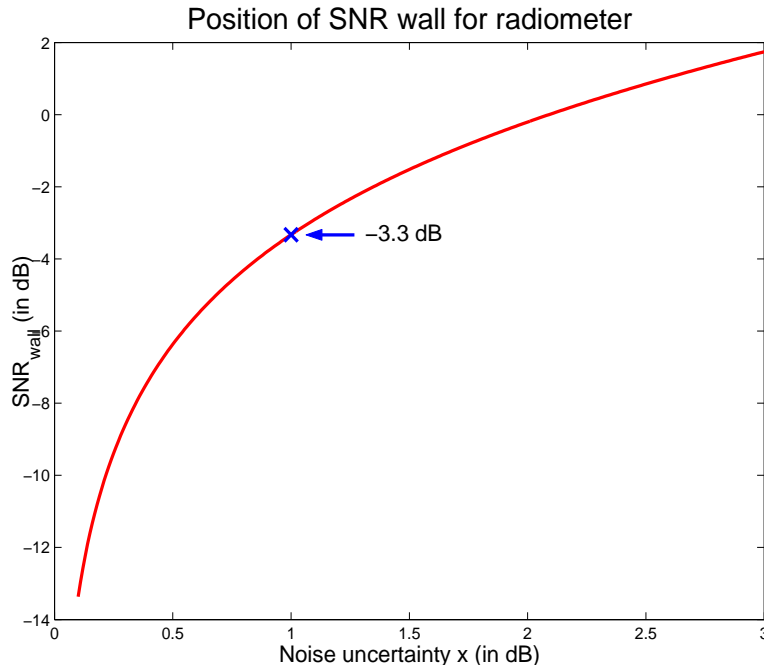


Fig. 13. This figure plots the  $SNR_{wall}$  for the radiometer as a function of noise level uncertainty  $x$  where  $\alpha = 10^{x/10}$  and  $\sigma_{low}^2 = \frac{1}{\alpha}$  and  $\sigma_{high}^2 = \alpha$ . The point marked by a “x” on the plot corresponds to 1 dB of device level noise uncertainty. The position of the SNR wall at this value of noise uncertainty is approximately -3 dB. This shows that the radiometer is highly non-robust, even to simple device noise level uncertainties.

- Even moments of the noise must be close to the nominal noise moments in that  $\mathbb{E}W_a^{2k} \in [\frac{1}{\alpha^k} \mathbb{E}W_n^{2k}, \alpha^k \mathbb{E}W_n^{2k}]$ , where  $W_n$  is the nominal noise random variable and  $\alpha = 10^{x/10} > 1$ .

Under this noise uncertainty model<sup>5</sup> we can derive the following result:

**Theorem 2:** Consider detection of the presence or absence of the i.i.d. signal  $X[n]$ , which are zero-mean, drawn from a known signal constellation signal with low amplitude, and are corrupted by additive noise whose distribution may lie in  $\mathcal{W}_x$ .

In this case we show that there exists an  $SNR$  threshold, say  $SNR_{wall}^*$  below which it is impossible to robustly detect the signal irrespective of the decision strategy used. We also give a characterization of  $SNR_{wall}^*$  as a minimization of sequence of  $SNR$  thresholds for the moment

<sup>5</sup>An alternative, equivalent, and more intuitive model is depicted in Figure 14.

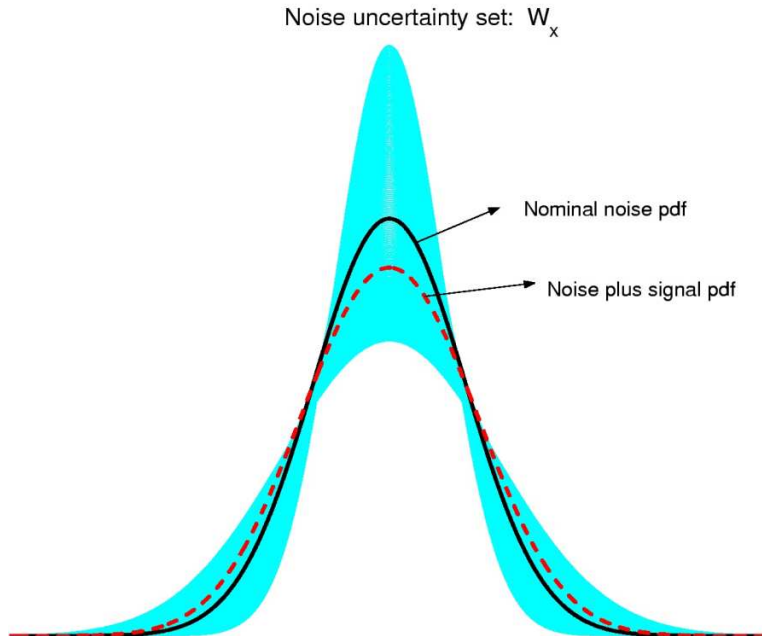


Fig. 14. An example of the noise uncertainty set,  $\mathcal{W}_x$ . The shaded region is the set of all possible pdfs for the noise random variable. This region has been constructed as an envelope of all the pdfs of Gaussian random variables with variance in the range  $\frac{1}{2}\sigma^2, 2\sigma^2$ . The bold curve inside the region is the pdf of a nominal Gaussian,  $W_n$ . The dashed curve is the pdf of  $X + W_n$  for the case when  $X$  is BPSK modulated at  $SNR = -6dB$ . It is clear from this example that at low signal powers, the pdf of signal plus noise falls within the noise uncertainty set and hence the signal cannot be differentiated from noise.

detectors<sup>6</sup>.

*Proof:* To prove the above result, we need to show the following equivalence

$$\text{Robust detection is impossible for every detector} \Leftrightarrow SNR \leq SNR_{wall}^*$$

We prove the above equivalence by separately proving the following. We show that there exists an  $SNR_{wall}^*$  such that

$$SNR \leq SNR_{wall}^* \stackrel{(a)}{\Rightarrow} \text{robust detection is impossible}$$

$$\text{Robust detection is impossible} \stackrel{(b)}{\Rightarrow} SNR \leq SNR_{wall}^*$$

<sup>6</sup>Throughout this theorem we work with the peak signal to noise ratio, rather than the average signal to noise ratio. This is done for make the mathematical analysis easier. Note that there is not too much loss of generality in this assumption, because for signal constellations with low signal amplitude, the peak  $SNR$  is also bounded and hence is not too much higher than the average signal to noise ratio.

**Proof of (a):** Let  $W_n \sim \mathcal{N}(0, \sigma^2)$ ,  $W_1 \sim \frac{1}{\sqrt{\alpha}}W_n$  and  $X \sim X[n]$ . Now, define a new random variable  $W_2 := X + W_1$ . By definition,  $W_1 \in \mathcal{W}_x$ , and if  $W_2 \in \mathcal{W}_x$ , then it is clear that robust detection is impossible. Since,  $\mathbb{E}W_2^{2k} \geq \mathbb{E}W_1^{2k}$  for  $k = 1, 2, \dots$ ,  $W_2 \in \mathcal{W}_x$  iff

$$\begin{aligned}
& \mathbb{E}W_2^{2k} \leq \alpha^k \mathbb{E}W_n^{2k} \\
\Leftrightarrow & \mathbb{E}(X + W_1)^{2k} \leq \alpha^k \mathbb{E}W_n^{2k} \\
\Leftrightarrow & \frac{\mathbb{E}(X + W_1)^{2k}}{\mathbb{E}W_n^{2k}} \leq \alpha^k \\
\Leftrightarrow & \sum_{i=1}^k \binom{2k}{2k-2i} \left(\frac{1}{\alpha^{k-i}}\right) \frac{\mathbb{E}W_1^{2k-2i}}{\mathbb{E}W_n^{2k}} \mathbb{E}X^{2i} \leq \alpha^k \\
\Leftrightarrow & \sum_{i=0}^k \binom{2k}{2k-2i} \left(\frac{1}{\alpha^{k-i}}\right) \left(\frac{1 \cdot 3 \cdot 5 \cdots (2k-2i-1) \sigma^{2k-2i}}{1 \cdot 3 \cdot 5 \cdots (2k-1) \sigma^{2k}}\right) \mathbb{E}X^{2i} \leq \alpha^k \\
\Leftrightarrow & \sum_{i=0}^k \binom{2k}{2k-2i} \left(\frac{1}{\alpha^{k-i}}\right) \left(\frac{1 \cdot 3 \cdot 5 \cdots (2k-2i-1)}{1 \cdot 3 \cdot 5 \cdots (2k-1)}\right) \frac{\mathbb{E}X^{2i}}{\sigma^{2i}} \leq \alpha^k \\
\Leftrightarrow & \sum_{i=0}^k \binom{2k}{2k-2i} \left(\frac{1}{\alpha^{k-i}}\right) \left(\frac{1 \cdot 3 \cdot 5 \cdots (2k-2i-1)}{1 \cdot 3 \cdot 5 \cdots (2k-1)}\right) SNR^i \leq \alpha^k \quad \forall k = 1, 2, \dots \quad (8)
\end{aligned}$$

Note that, we need to assume  $\frac{\mathbb{E}X^{2i}}{\sigma^{2i}} \leq SNR^i$  in order to justify the penultimate step in the chain of inequalities used above. This is true since we are considering peak signal to noise ratio, rather than the average signal to noise ratio. However, there is no big loss of generality while working with the peak  $SNR$  because we are dealing with signals whose amplitude is considerably less than the noise power. Hence, both the average and peak signal to noise ratio is very very low.

Now, for a fixed  $k$ , consider the equation

$$f(k, SNR) := \left[ \sum_{i=0}^k \binom{2k}{2k-2i} \left(\frac{1}{\alpha^{k-i}}\right) \left(\frac{1 \cdot 3 \cdot 5 \cdots (2k-2i-1)}{1 \cdot 3 \cdot 5 \cdots (2k-1)}\right) SNR^i \right] = \alpha^k \quad (9)$$

The LHS of (9),  $f(k, SNR)$ , is a degree  $k$  polynomial in one variable,  $SNR$ , with positive coefficients. Also,  $f(k, SNR)$  is monotonically increasing in  $SNR$  for a fixed  $k$ . Hence, it is clear that the (9) will have a unique positive solution. Call it  $SNR_{wall}^{(2k)}$ . From the monotonicity of  $f(k, SNR)$  we have,

$$f(k, SNR) \leq \alpha^k \quad \text{if} \quad SNR \leq SNR_{wall}^{(2k)}$$

Now, define  $SNR_{wall}^*$  by

$$SNR_{wall}^k := \inf_{k=1,2,3,\dots} SNR_{wall}^{(2k)} \quad (10)$$

From the definition it is clear that if  $SNR \leq SNR_{wall}^*$ , the inequality in (8) is satisfied for all  $k = 1, 2, \dots$ . Hence, robust detection is impossible if  $SNR \leq SNR_{wall}^*$ , which proves (a).

**Proof of (b):** Now suppose that robust detection is impossible for any detector. This implies that, there exists atleast two noise distributions  $W_1, W_2 \in \mathcal{W}_x$ , such that  $W_1 + X \sim W_2$ . In particular the above claim must also be true for  $W_1 \sim \frac{1}{\sqrt{\alpha}}W_n$ . This happens

$$\Leftrightarrow \mathbb{E}(W_1 + X)^{2k} = \mathbb{E}W_2^{2k} \quad \forall k = 1, 2, \dots$$

Dividing by  $\mathbb{E}W_n^{2k}$  on both sides we get

$$\frac{\mathbb{E}(W_1 + X)^{2k}}{\mathbb{E}W_n^{2k}} = \frac{\mathbb{E}W_2^{2k}}{\mathbb{E}W_n^{2k}} \quad \forall k = 1, 2, \dots$$

Expanding  $\mathbb{E}(W_1 + X)^{2k}$ , we get

$$\begin{aligned} \sum_{i=0}^k \binom{2k}{2k-2i} \left(\frac{1}{\alpha^{k-i}}\right) \left(\frac{1 \cdot 3 \cdot 5 \cdots (2k-2i-1)}{1 \cdot 3 \cdot 5 \cdots (2k-1)}\right) SNR^i &= \frac{\mathbb{E}W_2^{2k}}{\mathbb{E}W_n^{2k}} \\ \sum_{i=0}^k \binom{2k}{2k-2i} \left(\frac{1}{\alpha^{k-i}}\right) \left(\frac{1 \cdot 3 \cdot 5 \cdots (2k-2i-1)}{1 \cdot 3 \cdot 5 \cdots (2k-1)}\right) SNR^i &\leq \alpha^k \quad \forall k = 1, 2, \dots \end{aligned} \quad (11)$$

which is exactly identical to (8). Hence we must have  $SNR \leq SNR_{wall}^*$ , which proves the claim. ■

### C. Bounds on the $SNR_{wall}^*$

From theorem 2, we know that there exists an  $SNR$  threshold,  $SNR_{wall}^*$ , below which robust detection is absolutely impossible. However, the result is vacuous if  $SNR_{wall}^* = 0$ . This can happen if the infimum in (10) is zero. In this section we actually compute bounds on  $SNR_{wall}^*$  and illustrate using numerical computations to show that the bounds are tight.

Recall that  $SNR_{wall}^k := \inf_{k=1,2,3,\dots} SNR_{wall}^{(2k)}$  and hence,  $SNR_{wall}^* \leq SNR_{wall}^{(2)}$ . Therefore we have the obvious upper bound on the  $SNR$  wall,

$$SNR_{wall}^* \leq SNR_{wall}^{(2)} = \frac{\alpha^2 - 1}{\alpha} \quad (12)$$

Obtaining a lower bound is a bit more challenging. Recall that  $SNR_{wall}^{(2k)}$  is the root of the polynomial  $f(k, SNR) - \alpha^k$ . The coefficient of  $SNR^i$  in  $f(k, SNR) - \alpha^k$  is  $\binom{2k}{2k-2i} \left(\frac{1}{\alpha^{k-i}}\right) \left(\frac{1 \cdot 3 \cdot 5 \cdots (2k-2i-1)}{1 \cdot 3 \cdot 5 \cdots (2k-1)}\right)$ . We now replace  $\left(\frac{1}{\alpha^{k-i}}\right)$  by 1 in the coefficient of  $SNR^i$  to get a new polynomial,  $\tilde{f}(k, SNR) - \alpha^k$ .

Since  $\alpha > 1$ , we have  $(\frac{1}{\alpha^{k-i}}) \leq 1$  for all  $i = 1, 2, \dots, k$ , and hence the unique positive root of  $\tilde{f}(k, SNR) - \alpha^k = 0$  must be smaller than  $snr_{wall}^{(2k)}$ . Call this root  $S\tilde{N}R_{wall}^{(2k)}$ . Therefore, we have

$$\begin{aligned} SNR_{wall}^{(2k)} &\geq S\tilde{N}R_{wall}^{(2k)} \\ \Rightarrow \inf_{k=1,2,\dots,\infty} SNR_{wall}^{(2k)} &\geq S\tilde{N}R_{wall}^{(2k)} \\ \Rightarrow SNR_{wall}^* &\geq S\tilde{N}R_{wall}^{(2k)} \\ \Rightarrow SNR_{wall}^* &\geq \inf_{k=1,2,\dots,\infty} S\tilde{N}R_{wall}^{(2k)} \end{aligned}$$

This gives us a lower bound on  $SNR_{wall}^*$ ,

$$SNR_{wall}^* \geq \inf_{k=1,2,\dots,\infty} S\tilde{N}R_{wall}^{(2k)} \quad (13)$$

where  $S\tilde{N}R_{wall}^{(2k)}$  is the unique positive root of

$$\tilde{f}(k, SNR) := \left[ \sum_{i=0}^k \binom{2k}{2k-2i} \left( \frac{1 \cdot 3 \cdot 5 \cdots (2k-2i-1)}{1 \cdot 3 \cdot 5 \cdots (2k-1)} \right) SNR^i \right] = \alpha^k \quad (14)$$

Our problem is not yet completely solved, because the lower bound for  $SNR_{wall}^*$  is yet another optimization problem, and it is hard to get a closed form solution for  $S\tilde{N}R_{wall}^{(2k)}$ . However, this optimization problem is easier than the first one and we can show that,  $\inf_{k=1,2,\dots,\infty} S\tilde{N}R_{wall}^{(2k)} = S\tilde{N}R_{wall}^{(2)} = \alpha - 1$ . Hence, we have

$$\alpha - 1 \leq SNR_{wall}^* \leq \frac{\alpha^2 - 1}{\alpha} \quad (15)$$

The comparison of these bounds is illustrated in Figure 15. The true wall lies somewhere in between. The tightness of our bounds is obvious from the figure.

#### D. Detector robustness: coherent case

Many signals contain deterministic pilot tones that we can try to coherently detect. Relative to the radiometer, there is some loss since the pilot tone only has a fraction of the total signal power. At low SNR, this loss is offset by the coherent processing gain which grows with dwell time. Here, we analyze the coherent detector in brief and evaluate its robustness under different uncertainties.

For simplicity, assume the primary's signal is given by  $\sqrt{\theta}X_p[n] + \sqrt{(1-\theta)}X[n]$ . Here  $X_p[n]$  is a known pilot tone with  $\theta$  being the total fraction of energy allocated to the pilot tone and

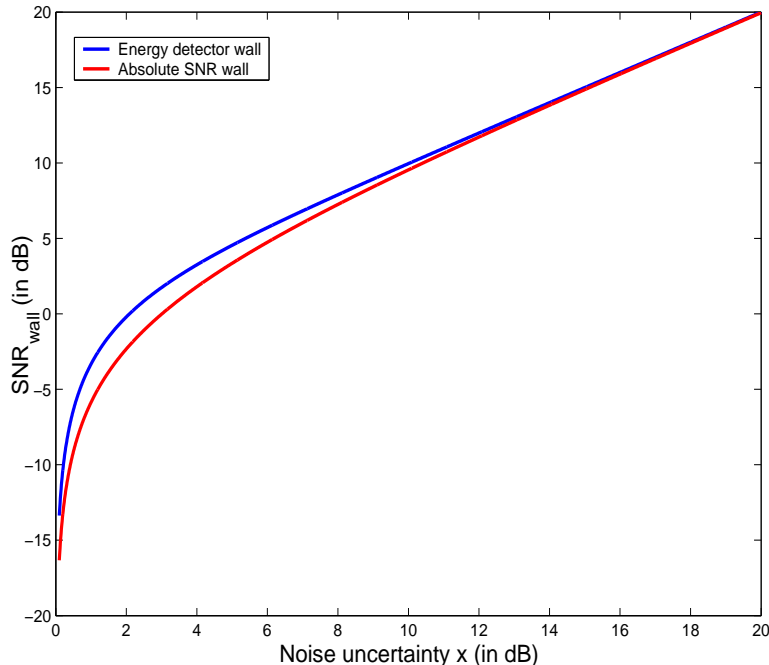


Fig. 15. This figure plots the upper (top curve) and lower bound (bottom curve) for  $SNR_{wall}^*$ , as a function of noise uncertainty  $x$ . This figure was obtained by using the bounds derived in (15). The figure also compares the absolute  $SNR$  wall to the  $SNR$  wall for the energy detector (top curve). It is clear from the figure that almost every non-coherent detector suffers as badly as the radiometer under noise level uncertainties.

$X[n]$ ,  $W[n]$  are i.i.d. as before. It is known that in the simple case of completely known noise statistics and no uncertainties in the system, the matched filter is asymptotically optimal. It achieves a dwell time  $N \approx [\mathcal{Q}^{-1}(P_D) - \mathcal{Q}^{-1}(P_{FA})]^2 \theta^{-1} SNR^{-1}$  [25].

Now suppose that the noise variance lies in  $[\sigma_{low}^2, \sigma_{high}^2]$ . The test statistic for the coherent detector is  $T(\mathbf{y}) = \frac{1}{\sqrt{N}} \sum_{n=1}^N Y[n] \hat{X}_p[n]$ , where  $\hat{\mathbf{x}}_p$  is a unit vector in the direction of the pilot tone. This averages out the noise in other orthogonal directions and the new noise uncertainty set is  $[\frac{\sigma_{low}^2}{N}, \frac{\sigma_{high}^2}{N}]$ , which shrinks to zero as  $N \rightarrow \infty$ . By dwelling long enough, the primary signal strength becomes greater than the uncertainty in the noise and hence there is no wall. Enough coherent processing gain can turn a low SNR situation into a high SNR one.

Incorporating multipath into our model, the primary signal in (1) is given by  $\sum_{l=0}^{L-1} h_l[n] \tilde{X}[n-l]$ , where  $\tilde{X}[n] = \sqrt{\theta} X_p[n] + \sqrt{(1-\theta)} X[n]$ , and  $h_l[n]$  are the multipath fading coefficients<sup>7</sup>.

<sup>7</sup>Note that the channel taps cannot be estimated at the cognitive radio receiver since we are not yet sure if the primary signal is even ON or OFF. The signal strength is too low to get an accurate estimate.

As before, assume that the noise level is uncertain though white, i.e.,  $W[n]$  lies in the noise uncertainty set  $\mathcal{W}_x$ .

In this case it is clear that we cannot reap the gains of coherent signal processing forever. As soon as the channel taps assume independent realizations, we can no longer gain from coherent signal processing. Detector performance depends on the channel coherence time,  $T_c$ <sup>8</sup>. For simplicity, assume that the coherence time is known at the cognitive radio's sensor.

The asymptotically optimal test statistic is  $T(\mathbf{y}) = \frac{1}{M} \sum_{n=0}^{M-1} \left[ \frac{1}{\sqrt{N_c}} \sum_{k=1}^{N_c} Y[n] \hat{X}_p[nN_c + k] \right]^2$ , where  $N_c$  is the number of samples in each coherent block and  $M$  is the number of coherent blocks over which we listen for the primary. This detector can be visualized as a combination of two detectors. First, the signal is coherently combined within each coherence time  $T_c$ . Coherent processing gain boosts the signal by  $N_c$  while the noise uncertainty is unchanged. Second, the new boosted signal is detected at the receiver by passing it through a radiometer.

The radiometer aspect remains non-robust to noise uncertainties, in spite of the boost in the signal strength. However, the robustness is improved and the  $SNR$  wall is lowered by a factor of  $10 \log_{10} N_c$  dB.

Coherent processing gains could also be limited due to implementational complexity. The clock-instability of both the sensing radio and the primary transmitter imposes a limit on the coherent processing time. For instance, suppose that there is 1000 Hz of frequency uncertainty and we are doing coherent processing over 1 ms. Since the pilot frequency is uncertain, suppose that we need to search over 4 bins to achieve a target probability of missed detection. If we want to do coherent processing over 10 ms, we now need to search over 40 frequency bins. Since searching over frequency bins involves computing FFTs, it is clear that the coherent processing time is limited by the complexity of the cognitive radio receiver. Finally, coherent processing gains might be limited due to the lengths of the pilots themselves. In OFDM-based primary systems, the pilots are embedded within each packet and are only coherent for a packet duration. No further coherent processing gain is available.

<sup>8</sup>Here channel coherence time is defined as the time for which the channel taps remain approximately constant [29].

### E. Detector robustness: feature detectors

We now consider the case when the primary signal is no longer white.<sup>9</sup> In that case, it is possible to use cyclostationary feature detectors to exploit the colored nature of the signal [30], [31]. These detectors can be expressed in terms of a quadratic transformation on the received signal  $y(t)$ :  $T(\mathbf{y}(t)) = \int_{t-T/2}^{t+T/2} \int_{t-T/2}^{t+T/2} k(u, v)y(u)y^*(v)dudv$  for some kernel  $k(u, v)$  [30]. Since these transformations are quadratic, their sample complexity is  $O(SNR^{-2})$ . In terms of robustness, they are similar to coherent detectors. The transformed signal  $T(\mathbf{y}(t))$  has non-zero mean under the signal present case ( $\mathcal{H}_1$ ) and has zero-mean when the signal is absent ( $\mathcal{H}_0$ ). The quadratic transformation converts the non-coherent problem into a coherent problem, at the expense of a “squaring loss.” These detectors gain some robustness to noise level uncertainties, but remain non-robust to the coherence-time related uncertainties of Section II-D.

Furthermore, in such cases, it is also important to remember that the bounds are optimistic since the physical noise is only approximately white. After all, it reflects the sum of many different physical sources of undesired signals, not all of which are white! Even without motion, for low enough SNR, the structure brought by the signal will be indistinguishable from the uncertain low level structure of the noise.

### F. Interference estimation improves detector robustness

Theorem 2 shows that the  $SNR_{wall}$  is a function of the uncertainty in the noise at the receiver. Once we leave the exclusive use model, the amount of interference from other opportunistic cognitive radio systems is a major source of uncertainty. This imposes severe limitations on the ability to sense primary transmissions. In order to improve detector robustness, it is clear that we need to estimate the interference from the secondary transmissions.<sup>10</sup>

The spectrum is broken up into different chunks of bandwidth and is assigned to primary users by the FCC. For traditional robustness reasons, small guard bands (see Figure 16) between these spectrum chunks are left unassigned. We can use these guard bands to estimate<sup>11</sup> the

<sup>9</sup>e.g. we sample it faster than the Nyquist rate and include a wider band around the signal.

<sup>10</sup>As well as any “self-interference” of  $X[n]$  with  $X_p[n]$  that may exist in the coherent case.

<sup>11</sup>The goal is to estimate the average power of the interference, not necessarily to estimate its exact value. If the interfering signal is information bearing, estimating its exact value is likely to be impossible unless we can decode it. Even then, [32] reveals that some prediction error is left.

interference (see Figure 17). The problem is that the interference estimate in the guard bands is not a very accurate estimate of the interference within the band itself. A lot of uncertainty remains. However, if the sensor is trying to detect a pilot tone, then the estimation error can be reduced considerably.

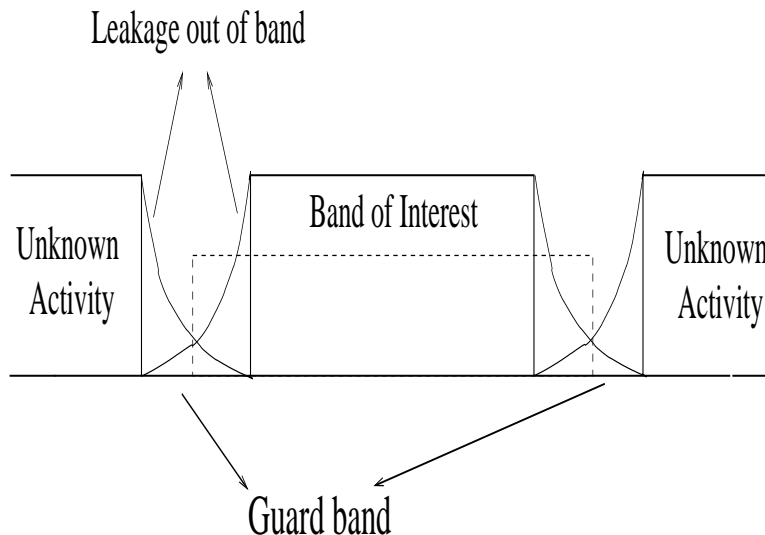


Fig. 16. Guard band measurements can help estimate interference. The guard bands have leakages from adjacent bands which affect our interference estimate. Also, the estimate depends on the frequency selectivity of the secondary transmissions. For example, some secondary systems might be transmitting OFDM packets, in which case the interference varies with the frequency of the subcarriers used. So, the measurement in the guard band may or may not be a good estimate of the interference in the center of the primary band. To summarize, our guard band measurements are very good estimates for interference at the edge of the band of interest, and the estimate gets worse as we go farther away from the edge of the primary band.

It is clear that the quality of the estimate depends on the correlation of the interference power across frequencies. To ensure that the interference estimate does not contain the pilot tone itself, the estimation must be based on measurements at frequencies larger than the possible Doppler spread,  $D_s$ , of the primary-secondary channel as well as the uncertainty in the clock frequency.<sup>12</sup> Meanwhile, the reference measurements must be within the coherence bandwidth,  $W_c$ , of the secondary-secondary channels to ensure that the interference does not change too much (see Figure 40). However, since most of the interfering radios are likely nearby, the delay spread  $T_d$  of the channel is low and hence  $W_c \approx \frac{1}{T_d} \gg \max(D_s, \text{frequency uncertainty})$ . Therefore, the

<sup>12</sup>In most cases the frequency uncertainty is larger than the Doppler spread.

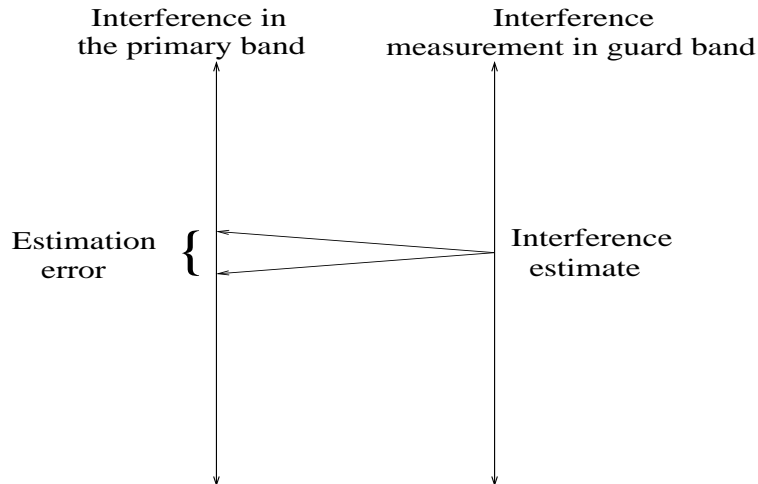


Fig. 17. Interference estimation via guard band measurements. By measuring the energy in the guard bands adjacent to the ‘band of interest’ we can get an estimate of the noise plus interference. This can possibly reduce uncertainty in the level of interference. In most situations 10% may be a good guess for the estimation error.

interference estimate is likely to be quite accurate assuming that the interference signals look white on this scale.<sup>13</sup>

### III. POWER CONTROL

Non-interference to the primary system is the fundamental constraint on any system of secondary use. For a secondary transmitter, this translates to a limit on its maximum transmit power. This limit depends on several factors, including the secondary user’s distance from the primary receivers, signal attenuation rates, and the presence or absence of multiple secondary transmitters. We assume that the relative positions of the primary and secondary transmitters are unknown. Thus, the secondary node must control its power based on what it senses. The power of the primary signal must act as a proxy for the distance.

We begin by considering a single secondary user sharing spectrum with the primary system. The single secondary user regime is split further into two subcases. We can think of the secondary

<sup>13</sup>This may not be a good assumption on the relevant time scale. If the total time for coherent processing will include only a few packets from any given nearby secondary using an OFDM style system, then the dominant uncertainty is actually the local non-whiteness of the interference on this time-scale. As a result, it is probably hopelessly optimistic to count on more than 10dB or so of a reduction in interference uncertainty from prediction.

users as licensed users constrained to a specific power. This could happen if two distinct property rights were auctioned off for a particular frequency band. For example, company A could purchase the right to transmit up to 10 kW on the 800-900 MHz band anywhere in the US. while company B could purchase the right to transmit up to 1 kW on the same band but only when A is not using it. On the other hand, it seems reasonable to allow a secondary user to use more power if he is further from the primary system.

We examine both these cases in section III-D, followed by the effects of shadowing/fading in section III-G. In section III-E, we extend our analysis to multiple secondary users. We consider first the case in which all the secondary users are bound by the same power constraint. Finally, in section III-E.2, we allow the secondary users to be heterogeneous in nature and to increase their transmit power with distance from the primary system. This final viewpoint more closely aligns with the traditional view of cognitive radio [18]. After first considering secondary users that increase their power without bound, we note that practical radios will have a minimum detectable SNR, so failure to detect a signal means only that the SNR has fallen below some threshold. This caps a cognitive radio's transmit power and is explored in section III-F.

#### A. Model

In our model, we assume a band already potentially assigned to a single-transmitter system. We are particularly interested in long-range primary transmissions such as television, but for the sake of comparison we also present examples involving a shorter-range primary such as a 802.11 wireless access point. Within some protected radius of the primary transmitter, all unshadowed primary receivers must be guaranteed reception, even when the cognitive radios are operating. All transmissions are assumed to be omnidirectional.

It should be mentioned that opportunistic devices must consider the leakage from their transmissions into adjacent bands. Since this leakage from the secondary transmitters will be much weaker than their in-band transmissions, the leakage will only be a problem if the systems on adjacent bands are significantly more sensitive to interference. The power control rule must be based on whichever band presents the most restrictive constraint.

In Section I-C we showed that secondary users must be able to coherently detect a known pilot signal or training sequence from the primary transmitter. If a training sequence is transmitted as part of the primary transmission, its SNR will be the same as the SNR of the data portion of

the transmission. We will make this assumption throughout this chapter.

However, the pilot signal case is more complicated. First of all, the pilot signal may be significantly weaker than the primary's data signal, perhaps 20 dB or more down. This will have the same result as insurmountable shadowing (section III-G), forcing secondary users to detect a 20 dB weaker signal. This effect will be clearly seen if the pilot is sent in a separate frequency band or time slot from the primary transmission. However, if the pilot signal and the primary data signal are sent in the same band, there will be a non-linear effect on the pilot signal's SNR due to interference from the data signal. Near the primary transmitter, the data signal will dominate the noise experienced by pilot signal detectors, making pilot signal SNR a poor proxy for distance. However, in this high SNR regime, the optimal detector (Section II) is a radiometer, not a coherent detector of a weak signal. The SNR of the entire primary transmission, not just the SNR of the pilot signal, would therefore be an appropriate proxy for distance. For secondary users far from the primary transmitter, especially in the middle of nowhere, the noise from the primary data signal will be significantly attenuated and be much weaker than the ambient noise. This non-linear effect will be addressed in future work.

### *B. SNR as a proxy for distance*

The primary system has a minimum required SINR to successfully decode at its target rate  $R$ . In the absence of interference, this  $\gamma_{dec}$  occurs at a radius  $r_{dec}$  from the transmitter. The idea is to guarantee service to primary users within some protected radius ( $r_p$ ) by defining an additional "no-talk radius" ( $r_n$ ) within which secondary users must be quiet (Figure 20). At distances from the primary transmitter greater than  $r_n$ , secondary users might be allowed to transmit. Ideally, these "no-talk regions" would be centered on each of the primary system's receivers, but we assume that the cognitive radios have no way of knowing these locations. The general situation is illustrated in Figure 18 with the worst case scenario depicted in Figure 19.

If there is uncertainty in the noise power, then we can choose  $r_{dec}$  first and set  $\sigma^2$  to the maximum tolerable noise at that radius. If the noise power crosses this threshold with the cognitive radios transmitting, then protected users at  $r_p$  could experience an outage. However, this noise event would cause an outage for primary users at  $r_{dec}$  even without the cognitive radios. We also assume that this  $\sigma^2$  is preprogrammed into the cognitive radio, so it does not need to be continually estimated. Designing radios to compensate for changing noise floors is a

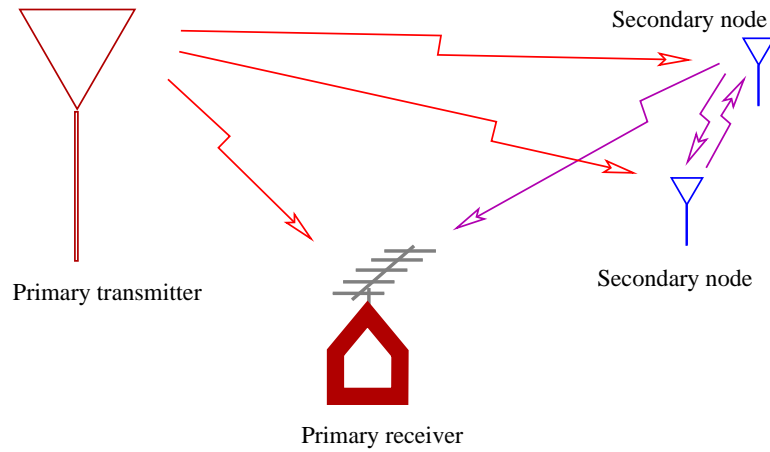


Fig. 18.

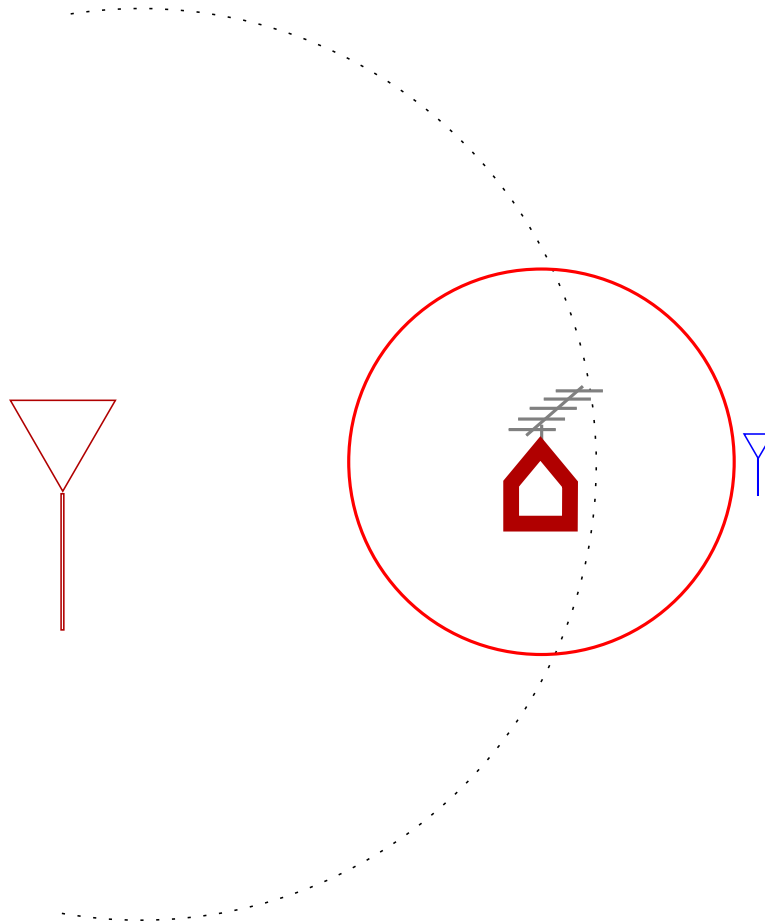


Fig. 19. Without knowledge of the primary receivers' locations, a secondary user must assume a worst-case scenario - that a primary receiver exists right on the border of the protected region. To be sure he is outside the primary receiver's required no-talk radius, the secondary user must be able to detect a weak signal.

topic for future research.

Since we are using locally measured SNR as a proxy for distance, it is convenient to represent the decodable radius  $r_{dec}$ , the protected radius  $r_p$ , and the location  $r_2$  of a secondary user in terms of the SNR in dB measured at those points. However, if the primary receiver is a TV antenna on a roof, it might measure an SNR of 0 dB at one location, while a cognitive radio on the ground at the same location might measure -10 dB. Therefore we must specify who is measuring the SNR at each distance. We consider  $\gamma_{dec}$  and  $\gamma_1$  to be measured by a primary receiver, while  $\gamma_2$  is measured by a secondary transmitter (Figure 20). We write the power of the secondary transmitter as  $P_2$ , and the power of the noise at the primary receiver  $\sigma^2$ .

Denoting the power of the primary transmitter as  $P_1$ , and the power of the noise at the primary receiver  $\sigma^2$ , we define:

$$\Delta \triangleq 10 \log \left( \frac{P_1}{\sigma^2} \right) - \gamma_{dec}$$

$$\mu \triangleq \gamma_1 - \gamma_{dec}$$

$$\psi \triangleq \gamma_{dec} - \gamma_2$$

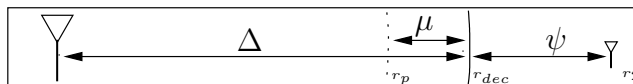


Fig. 20.

For example, if the minimum decodable SNR for the primary receiver is 10 dB and a secondary transmitter measures an SNR of -5 dB at  $r_n$ , then  $\psi = 15$ . We also define  $\psi$  to be the margin between  $\gamma_{dec}$  and the local SNR measured by a particular secondary user. Table II gives examples of how signal strengths map to distances.

As in [33], we represent the propagation-related power attenuation between two users a distance  $r$  apart as a function  $g(r)$  defined on  $[0, \infty]$ . We allow different gain functions  $g_{11}(r)$ , the propagation path loss between the primary transmitter and primary receiver,  $g_{12}(r)$ , between the primary transmitter and secondary receiver, and  $g_{21}(r)$ , between the secondary transmitter and primary receiver. Throughout this paper, our examples will be  $g_{11}(r) = g_{12}(r) = r^{-\alpha_1}$  and  $g_{21}(r) = r^{-\alpha_2}$ .

For example, for the gain function  $g_{11}(r) = r^{-3.5}$ ,  $\Delta = 165$  corresponds to a transmitter with about a 52 km range:

$$\Delta = 165 = 10 \log \left( \frac{P_1}{\sigma^2} \right) - 10 \log \left( \frac{P_1 r_{dec}^{-4}}{\sigma^2} \right)$$

$$r_{dec} = 10^{\frac{165}{3.5-10}} \approx 51800 \quad (16)$$

Further, consider  $\mu = 1$  dB and  $\psi = 0.01$  dB as potential operating margins. In this case,  $r_{dec} - r_p \approx 3300$  m, while  $r_n - r_{dec} \approx 34$  m. Because of the large protected radius, very small increments in dB correspond to large physical distances. This is important, because it means that the necessary operating margins can be quite small (Table II). Unless otherwise specified, we will assume  $\mu = 1$  for our plots.

Our assumption of a 52 km decodability radius is actually quite conservative. KRON-TV in San Francisco has an effective service radius of approximately 120 km [34], [35]. Furthermore, attenuation slower than  $r^{-4}$  causes small SNR margins to correspond to even greater distances. The magnitude of these differences makes it clear that an accurate model will be essential when designing practical cognitive systems.

	Attenuation as $r^{-4}$			Attenuation as $r^{-2}$		
	$r_{dec}$	$\psi = 1$ dB	$\psi = 0.01$ dB	$r_{dec}$	$\psi = 1$ dB	$\psi = 0.01$ dB
$\Delta = 50$ dB	18 m	1 m	0.01 m	320 m	39 m	0.36 m
$\Delta = 100$ dB	320 m	19 m	0.18 m	100,000 m	12,000 m	120 m
$\Delta = 150$ dB	5600 m	330 m	32 m	32,000,000 m	3,800,000 m	36,000 m

TABLE II

FOR LARGE  $\Delta$  (LARGE PRIMARY TRANSMIT DISTANCES) SMALL SNR MARGINS CORRESPOND TO LARGE PHYSICAL DISTANCES. IF THE SIGNAL ATTENUATES AS  $r^{-2}$  (AS COMPARED TO  $r^{-4}$ ) THE DISTANCES ARE EVEN LARGER.

Uncertainty in the attenuation model can be compensated for by using the most binding constraint. Opportunistic devices will be most restricted if the primary signal decays rapidly and the secondary signals decay slowly. An exponential attenuation model [36] captures this effect nicely and is addressed in greater detail in VI.

### C. Out-of-system interference

The interference from the secondary systems will be greatest to a user at the edge of the protected radius  $r_p$  (Figure 21).

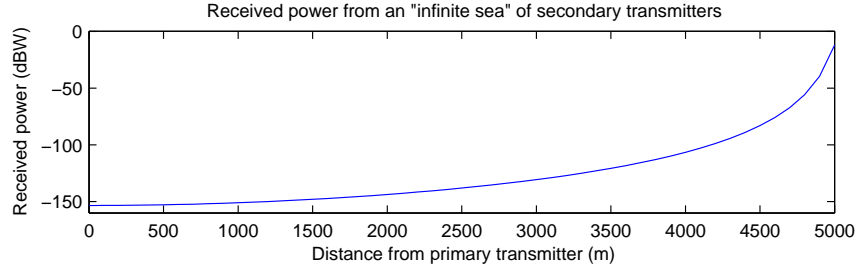


Fig. 21. Interference from secondary transmitters increases towards the border of the protected region. The secondary sea begins at 5100 m, at which point the interference becomes infinite.

That primary user has a maximum amount of out-of-system interference that it can tolerate. We examine the maximum allowable power for a secondary system while still guaranteeing decodability ( $\text{SINR} \geq \gamma_{dec}$ ) to a user on the protected border.  $Q_1$  and  $Q_2$  denote the primary and aggregate secondary transmitters' powers at the primary receiver, i.e.  $Q_1 = P_1 g_{11}(r_p)$  for a receiver on the edge of the protected region. A guarantee of reception can therefore be expressed as:

$$Q_2 + \sigma^2 \leq \sigma^2 10^{\frac{\mu}{10}} \quad (17)$$

We see that the secondary system must guarantee:

$$Q_2 \leq (10^{\frac{\mu}{10}} - 1)\sigma^2 \quad (18)$$

This is a fundamental constraint for any secondary system.

#### D. Single secondary transmitter

A one-size-fits-all power constraint must consider a primary receiver and secondary transmitter as close as possible, with the primary on the edge of the protected zone and the secondary on the edge of the no-talk zone. (18) implies:

$$\begin{aligned} P_2 g_{21}(r_n - r_p) &\leq (10^{\frac{\mu}{10}} - 1)\sigma^2 \\ P_2 &\leq (10^{\frac{\mu}{10}} - 1)\sigma^2 (g_{21}(r_n - r_p))^{-1} \end{aligned} \quad (19)$$

A more interesting case occurs when the single secondary transmitter is allowed to vary its power depending on its proximity to the protected region. We simply replace the worst case

distance  $r_n$  in equation (19) by the secondary's actual distance  $r_2$  from the primary transmitter. We observe that this new power schedule is strictly better than the “one-size-fits all” power limit because a secondary user on the edge of the no-talk region is now a worst case scenario. Since these distances are not known to the cognitive radio, we perform our calculations in terms of SNR.

First, we write  $r_p$ , the protected radius, in terms of SNR.

$$\begin{aligned} 10 \log \left( \frac{P_1}{\sigma^2} \right) - 10 \log \left( \frac{P_1 g_{11}(r_p)}{\sigma^2} \right) &= \Delta - \mu \\ g_{11}(r_p) &= 10^{\frac{-\Delta + \mu}{10}} \\ r_p &= g_{11}^{-1} \left( 10^{\frac{-\Delta + \mu}{10}} \right) \end{aligned} \quad (20)$$

Next, we solve for the distance  $r_2$  of the secondary transmitter, in terms of his local SNR.

$$\begin{aligned} 10 \log \left( \frac{P_1}{\sigma^2} \right) - 10 \log \left( \frac{P_1 g_{12}(r_2)}{\sigma^2} \right) &= \Delta + \psi \\ g_{12}(r_2) &= 10^{\frac{-\Delta - \psi}{10}} \\ r_2 &= g_{12}^{-1} \left( 10^{\frac{-\Delta - \psi}{10}} \right) \end{aligned} \quad (21)$$

Equations (20) and (21) let us write (19), the maximum allowable power for a secondary transmitter, in SNR terms.

$$\begin{aligned} \frac{P_2}{\sigma^2} &\leq (10^{\frac{\mu}{10}} - 1) (g_{12}(r_2 - r_p))^{-1} \\ &= \frac{(10^{\frac{\mu}{10}} - 1)}{(g_{21}(g_{12}^{-1}(10^{\frac{-\Delta - \psi}{10}})) - g_{11}^{-1}(10^{\frac{-\Delta + \mu}{10}}))} \end{aligned} \quad (22)$$

Alternatively, we can express how much more sensitive ( $\psi$  dB) secondary detectors must be than the primary receivers [37], [38]. The formula illustrates the idea that we must think in terms of distances, but calculate at the level of signal strengths. (See Figure 22)

$$\psi + \Delta \geq -10 \log_{10} [g_{11}(r_2)] \quad (23)$$

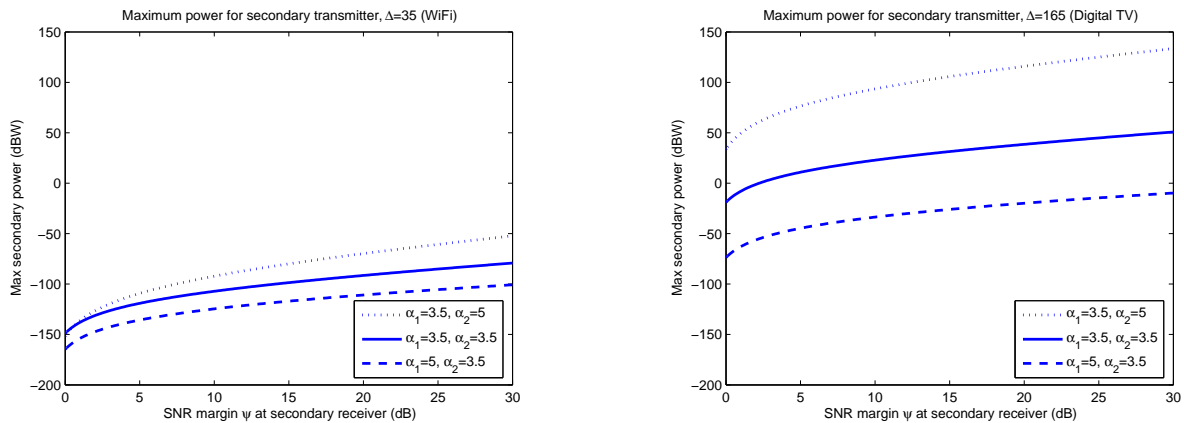
$$= -10 \log_{10} [g_{11}(r_{dec} + (r_2 - r_{dec}))] \quad (24)$$

$$= -10 \log_{10} \left[ g_{11} \left( g_{11}^{-1} \left( 10^{\frac{\mu - \Delta}{10}} \right) + g_{21}^{-1} \left( \frac{\sigma^2 \cdot (10^{\frac{\mu}{10}} - 1)}{P_2} \right) \right) \right] \quad (25)$$

For our example gain functions  $g_{11}(r) = g_{12}(r) = r^{-\alpha_1}$  and  $g_{21}(r) = r^{-\alpha_2}$  this gives us:

$$10 \log \left( \frac{P_2}{\sigma^2} \right) \leq \frac{\alpha_2}{\alpha_p} \Delta + 10 \log(10^{\frac{\mu}{10}} - 1) + 10\alpha_2 \log \left( \left( 10^{\frac{\psi}{10}} \right)^{\frac{1}{\alpha_p}} - \left( 10^{-\frac{\mu}{10}} \right)^{\frac{1}{\alpha_p}} \right) \quad (26)$$

The first term describes how aggressively the primary user is transmitting, i.e. how far a user can travel from the primary transmitter and still decode the signal. Increasing the primary transmitter's rate without increasing its power decreases  $\Delta$  and therefore requires the secondary transmitter to quiet down. The second term represents how tolerant the protected primary receivers are to interference. The final term represents how far the secondary transmitter is from the protected receivers. Also note that if  $\psi = -\mu$  the secondary transmitter is in the protected region and must be silent.



(a) Very low secondary powers when dealing with a weak primary user

(b) A lot more power is possible when primary is strong

Fig. 22. The graph illustrates the effect of different decay rates  $r^{-\alpha_1}$  and  $r^{-\alpha_2}$ . If  $\alpha_2 > \alpha_1$ , i.e. the secondary user's transmissions attenuate faster with distance than the primary transmissions do, we see the secondary user can use more power than he could if both systems experienced the same path loss.

If  $\alpha_2 > \alpha_1$ , i.e. the secondary user's transmissions attenuate faster with distance than the primary transmissions do, we see the secondary user can use more power than he could if both systems experienced the same path loss. This is likely to be the case, for example, if the primary transmitter is a tall TV antenna while the secondary users are located on the ground. The significance of the case in which  $\alpha_1 > \alpha_2$  will become apparent in Section III-E.

### E. Multiple secondary users

1) *Homogeneous secondary powers*: Suppose now that we are no longer limited to a single interferer. Outside of the no-talk circle of radius  $r_n$ , we assume there exists a sea of secondary transmitters, each with power  $P_2$ . Figure 23 illustrates a scenario in which there are many different secondary transmitters using a data-MAC protocol to spread out their active transmitters, implicitly enforcing a limit on the density of transmissions. Each secondary transmitter uniquely occupies a footprint of area  $A$ , so this “secondary sea” (Figure 24) has a power density  $D = \frac{P_2}{A}$ . Integrating over this sea gives the aggregate power of the secondary transmissions at a primary receiver on the edge of the protected region.

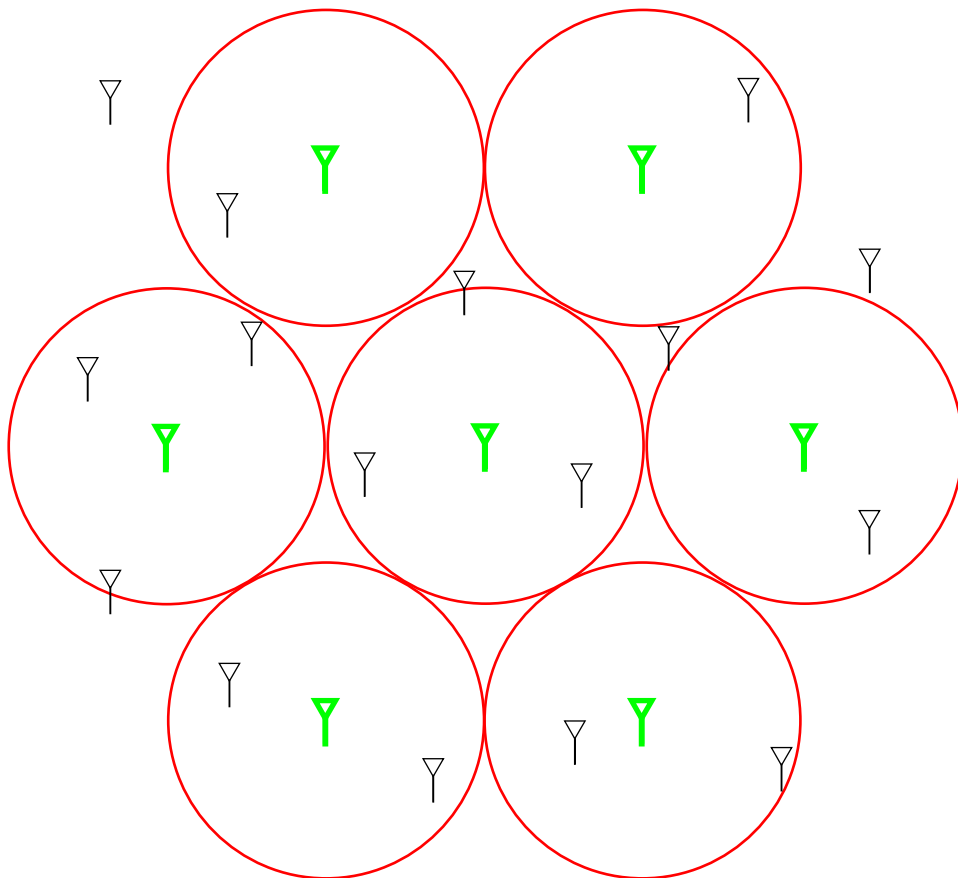


Fig. 23. Outside of the no-talk circle of radius  $r_n$ , we assume there exists a sea of secondary transmitters, each with power  $P_2$ . We further assume that there is a limit to how densely these transmitters are packed. Each secondary transmitter uniquely occupies a footprint of area  $A$ , so this “secondary sea” has a power density  $D = \frac{P_2}{A}$ . This density is implicitly created by any MAC protocol by limiting individual transmit powers and disallowing simultaneous transmissions within a transmitter’s footprint.

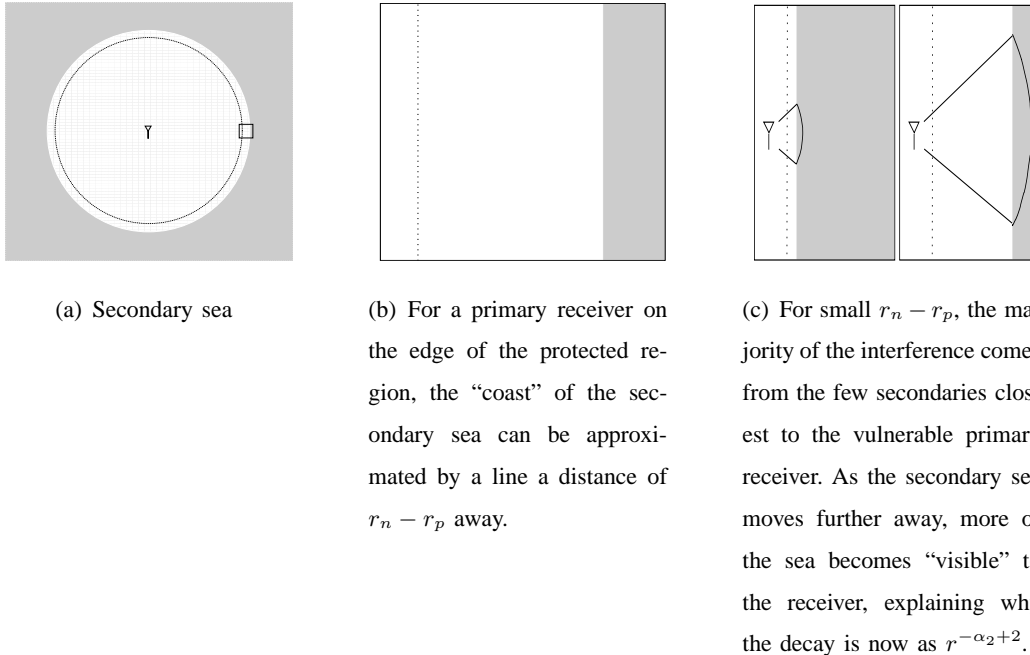


Fig. 24. The entire sea of secondary transmitters behaves like a single transmitter of power  $D \cdot K(\alpha_2)$ , located a distance  $r_n - r_p$  away (i.e. at the coast of the sea), but with a new decay exponent of  $-\alpha_2 + 2$ .

As in the case of the single licensed transmitter, we assume a constant power density outside the no-talk zone. Later, in section III-E.2, we will consider the case in which secondary users are allowed to increase the power of their transmissions as they venture further from the protected region.

We first assume that the secondary transmission power decays as  $g_{21}(r) = r^{-\alpha_2}$ ,  $\alpha_2 > 2$ . We also assume  $r_p \gg r_n - r_p$ , the distance between the primary receivers and the secondary transmitters. For a primary receiver on the edge of the protected region, the “coast” of the secondary sea can be approximated by a line a distance of  $r_n - r_p$  away. We examine the quality of this approximation in a later calculation (31).

$$\begin{aligned}
 Q_2 &= \int_{-\frac{\pi}{2}}^{\frac{\pi}{2}} \int_{\frac{r_n - r_p}{\cos(\theta)}}^{\infty} D r^{-\alpha_2} r \, dr \, d\theta \\
 &= \frac{D}{-\alpha_2 + 2} \int_{-\frac{\pi}{2}}^{\frac{\pi}{2}} \left[ r^{-\alpha_2 + 2} \right]_{\frac{r_n - r_p}{\cos \theta}}^{\infty} d\theta \\
 &= \frac{D \cdot (r_n - r_p)^{-\alpha_2 + 2}}{\alpha_2 - 2} \int_{-\frac{\pi}{2}}^{\frac{\pi}{2}} (\cos \theta)^{\alpha_2 - 2} d\theta
 \end{aligned} \tag{27}$$

$$= D \cdot K(\alpha_2) \cdot (r_n - r_p)^{-\alpha_2+2} \quad (28)$$

where  $K(\alpha_2) = \frac{\int_{-\frac{\pi}{2}}^{\frac{\pi}{2}} (\cos \theta)^{\alpha_2-2} d\theta}{\alpha_2-2}$ .

For  $\alpha_2 = 6$ ,  $K(\alpha_2) = \frac{1}{4} \frac{3!!}{4!!} \pi \approx 0.295$ .

The entire sea of secondary transmitters behaves like a single transmitter of power  $D \cdot K(\alpha_2)$ , located a distance  $r_n - r_p$  away (i.e. at the coast of the sea), but with a new decay exponent of  $-\alpha_2 + 2$ .

For small  $r_n - r_p$ , the majority of the interference comes from the few secondaries closest to the vulnerable primary receiver. As the secondary sea moves further away, more of the sea becomes “visible” to the receiver, explaining why the decay is now as  $r^{-\alpha_2+2}$ . The effect of increasing the secondary decay exponent by two is illustrated in Figure 22.

This approximation, however, understates the interference caused by the secondary sea in Figure 24a. We can upperbound the interference by considering the case where a primary receiver is completely surrounded by a secondary sea a distance  $r_n - r_p$  away. Using our generalized gain functions:

$$\begin{aligned} Q_2 &= \int_{-\pi}^{\pi} \int_{r_n-r_p}^{\infty} D \cdot g_{21}(r) r dr d\theta \\ &= D \int_{-\pi}^{\pi} [r\tilde{g}_{21}(r) - \check{g}_{21}(r)]_{r_n-r_p}^{\infty} d\theta \end{aligned}$$

where  $g_{21}(r) = \frac{d}{dr} \tilde{g}_{21}(r) = \frac{d^2}{dr^2} \check{g}_{21}(r)$ . Since  $g(r) \leq C \cdot r^{-2-\epsilon}$ ,  $\lim_{r \rightarrow \infty} (r\tilde{g}_{21}(r) - \check{g}_{21}(r)) = 0$  and it follows:

$$Q_2 = D \cdot 2\pi \cdot (\check{g}_{21}(r_n - r_p) - (r_n - r_p)\tilde{g}_{21}(r_n - r_p)) \quad (29)$$

Specifically, for our example gain functions, we have

$$I_{\text{aggregate}}(r) = D \cdot \frac{2\pi}{\alpha_2 - 2} \cdot (r_n - r_p)^{-\alpha_2+2} \quad (30)$$

$$= K(\alpha_{21})D(r_n - r)^{-\alpha_{21}+2} \quad (31)$$

Again, this bound claims that the sea behaves like a single transmitter of power located a distance  $r_n - r_p$  away but with a new decay exponent  $-\alpha_2 + 2$ . Figure 25 shows that the straight line approximation is quite good.

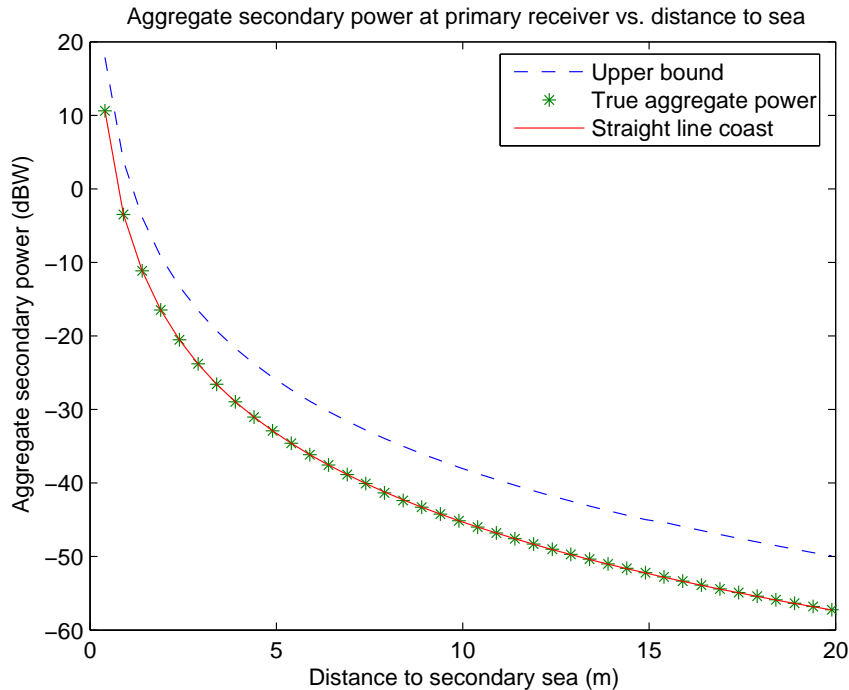


Fig. 25. The upper (eqn. 31) and lower (eqn. 28) bounds have the same decay exponent. Approximating the coast of the secondary sea with a straight line is accurate to within a constant.

2) *Heterogeneous secondary transmit powers*: We now consider the case in which secondary users are allowed to increase the power of their transmissions as they move further from the protected region. Clearly, the rule we pick to govern  $D(r)$  will determine the impact of the secondary sea on the primary receivers. Noting that  $\frac{1}{g_{21}(r)}$  is an increasing function, we assume the power density to be governed by a rule of the form:

$$D(r) = D_0(\rho) \frac{1}{g_{21}(r)} r^{-\rho} \quad (32)$$

where  $\rho$  is a constant that determines how aggressively the power density  $D(r)$  should increase with  $r$ . This rule can be expressed in terms of local SNR,  $\psi$ , in (37).

To determine the aggregate interference at a primary receiver on the edge of the protected region, we use the straight line approximation for the coast of the sea. For a particular  $\rho$ :

$$\begin{aligned}
Q_2 &= \int_{-\frac{\pi}{2}}^{\frac{\pi}{2}} \int_{\frac{r_n - r_p}{\cos(\theta)}}^{\infty} D(r) g_{21}(r) r dr d\theta \\
&= \frac{D_0(\rho)}{-\rho + 2} \int_{-\frac{\pi}{2}}^{\frac{\pi}{2}} [r^{-\rho+2}]_{\frac{r_n - r_p}{\cos \theta}}^{\infty} d\theta
\end{aligned} \tag{33}$$

If  $\rho > 2$ , i.e.  $D(r_2)$  grows sufficiently slower than  $g_{21}(r_2)$ , then the integral converges.

$$\begin{aligned}
&= \frac{D_0(\rho) \int_{-\frac{\pi}{2}}^{\frac{\pi}{2}} (\cos \theta)^{\rho-2} d\theta}{\rho - 2} (r_n - r_p)^{-\rho+2} \\
&= K(\rho) \cdot D_0(\rho) \cdot (r_n - r_p)^{-\rho+2}
\end{aligned} \tag{34}$$

With this particular rule for the power density, the sea of secondary transmitters behaves like a single transmitter located  $r_n - r_p$  from the protected radius, with power  $K(\rho) \cdot D_0(\rho)$  and gain function  $g_{21}(r) = r^{-\rho+2}$ . We can plug our expression straight into (25) to get an bound on  $D_0(\rho)$ .

$$D_0(\rho) \leq \sigma^2 \frac{(10^{\frac{\mu}{10}} - 1)}{K(\rho) \cdot (g_{12}^{-1}(10^{\frac{-\Delta-\mu}{10}}) - g_{11}^{-1}(10^{\frac{-\Delta+\mu}{10}}))^{-\rho+2}} \tag{35}$$

From (20) and (21) we can express  $r$  in terms of SNR:

$$r = r_2 - r_p = g_{12}^{-1}(10^{\frac{-\Delta-\psi}{10}}) - g_{11}^{-1}(10^{\frac{-\Delta+\mu}{10}}) \tag{36}$$

With (35) and (36) we can express (32) as a function of  $\psi$ :

$$\begin{aligned}
D(\psi) &= \sigma^2 \left( \frac{(10^{\frac{\mu}{10}} - 1)}{K(\rho) \cdot (g_{12}^{-1}(10^{\frac{-\Delta-\mu}{10}}) - g_{11}^{-1}(10^{\frac{-\Delta+\mu}{10}}))^{-\rho+2}} \right) \\
&\quad \left( \frac{(g_{12}^{-1}(10^{\frac{-\Delta-\psi}{10}}) - g_{11}^{-1}(10^{\frac{-\Delta+\mu}{10}}))^{-\rho}}{g_{21}(g_{12}^{-1}(10^{\frac{-\Delta-\psi}{10}}) - g_{11}^{-1}(10^{\frac{-\Delta+\mu}{10}}))} \right)
\end{aligned} \tag{37}$$

The kinds of tradeoffs possible are illustrated in Figure 26.

The primary receivers have a certain margin  $\mu$  of tolerable interference that through policy decisions can be allocated to users at different distances. The more aggressively (smaller  $\rho$ ) the secondary transmitters increase their power with distance, the quieter the secondary transmitters near the primary system must become. Heterogeneous secondary transmit powers can be accommodated, but policy decisions are necessary to set the tradeoff between sensed power and transmitted power. It can not be determined purely locally.

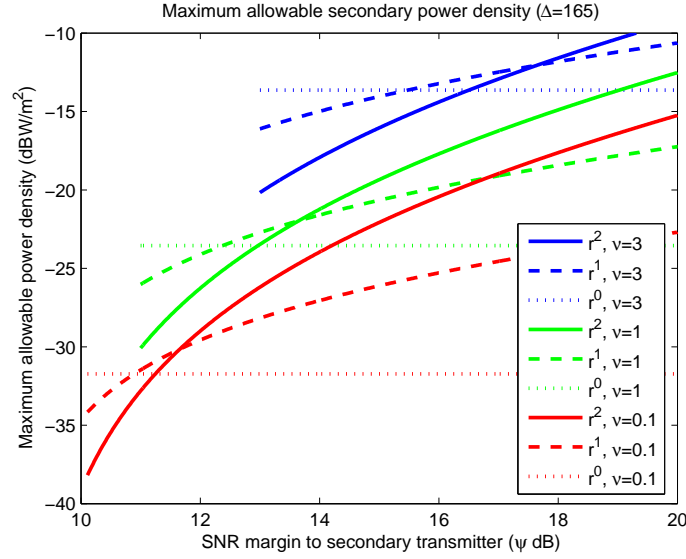


Fig. 26. The primary receivers have a certain margin  $\mu$  of tolerable interference that through policy decisions can be allocated to users at different distances. Nodes further from the primary system can transmit at greater powers, but only if nodes closer in transmit more quietly.

#### F. Minimum detectable SNR

In the preceding sections we mentioned an implicit cap on the transmit powers of the secondary users. Many factors contribute to this upper limit on power, including safety or hardware limitations. It is also affected by a radio's sensitivity:

As a secondary transmitter moves away from the protected radius, its allowable power increases exponentially. At some distance  $r_{max}$ , however, the local SNR at the secondary transmitter will drop below its minimum detectable SNR,  $\gamma_{min}$  [39]. From this point onwards, the secondary receiver cannot assume it is more than a distance  $r_{max}$  away from the transmitter, no matter what its actual distance. As a result, there is an absolute cap on the secondary transmit power. This in turn changes the aggregate interference at a primary transmitter on the border of the protected region.

$$\begin{aligned}
 Q_2 = & \int_{-\frac{\pi}{2}}^{\frac{\pi}{2}} \int_{\frac{r_n - r_p}{\cos(\theta)}}^{r_{max}} D(r) g_{21}(r) r dr d\theta \\
 & + \int_{-\frac{\pi}{2}}^{\frac{\pi}{2}} \int_{r_{max}}^{\infty} D(r_{max}) g_{21}(r) r dr d\theta
 \end{aligned} \tag{38}$$

$$\begin{aligned}
&= \frac{D_0}{-\rho + 2} \int_{-\frac{\pi}{2}}^{\frac{\pi}{2}} [r^{-\rho+2}]_{\frac{r_n - r_p}{\cos \theta}}^{r_{max}} d\theta \\
&\quad + \frac{D(r_{max})}{-\rho + 2} \int_{-\frac{\pi}{2}}^{\frac{\pi}{2}} [r\tilde{g}_{21}(r) - \check{g}_{21}(r)]_{r_{max}}^{\infty} d\theta \\
&= K(\rho) \cdot D_0 \cdot (r_n - r_p)^{-\rho+2} - \frac{D_0}{\rho - 2} \pi r_{max}^{-\rho+2} \\
&\quad + \frac{D(r_{max})}{\rho - 2} \pi [\check{g}_{21}(r_{max}) - r_{max}\tilde{g}_{21}(r_{max})] \tag{39}
\end{aligned}$$

We can express  $r_{max}$  in terms of  $\gamma_{min}$ .

$$\begin{aligned}
\gamma_{min} &= 10 \log \left( \frac{P_1 g_{12}(r_{max})}{\sigma^2} \right) - \beta \\
r_{max} &= g_{12}^{-1} \left( \frac{\sigma^2}{P_1} 10^{\frac{\gamma_{min} + \beta}{10}} \right) \tag{40}
\end{aligned}$$

We can use (39), (40), and (18) to find a bound on  $D_0$ . Alternatively, we could solve this expression for  $\gamma_{min}$ . If a manufacturer wanted to build cognitive radios that avoid interfering with legacy systems,  $\gamma_{min}$  represents how sensitive his radios' detection hardware must be.

### G. Shadowing/Fading

As shown in Figure 27, accounting for the possibility of  $\beta$  dB of shadowing/fading results in a pure shift of  $\beta$  in the required sensitivity of the opportunistic devices.

$$\psi \geq -10 \log_{10} \left[ \left( \frac{\sigma^2}{P_2} \cdot (10^{\frac{\mu}{10}} - 1) \right)^{-\frac{1}{\alpha_2}} + \left( 10^{\frac{\mu - \Delta}{10}} \right)^{-\frac{1}{\alpha_1}} \right]^{-\alpha_1} - \Delta + \beta \tag{41}$$

$$\tag{42}$$

However, choosing  $\beta$  requires more input. Inside the no-talk zone, secondary users will occasionally make a mistake and transmit even when it causes interfering with nearby primary systems. If the primary system is willing to tolerate a probability of harmful interference  $P_{HI}$  and there are  $K$  noncooperating secondaries, the probability of missed detection for any one secondary user must be less than  $P_{MD} = P_{HI}/K$  [40]. Figure 28 illustrates why the probability of a bad fade must be kept less than  $P_{MD}$ . Since  $P_{MD}$  is small, this requires a robust model for rare fades, which is going to be hopelessly conservative in most cases since rare fades can be very bad indeed.

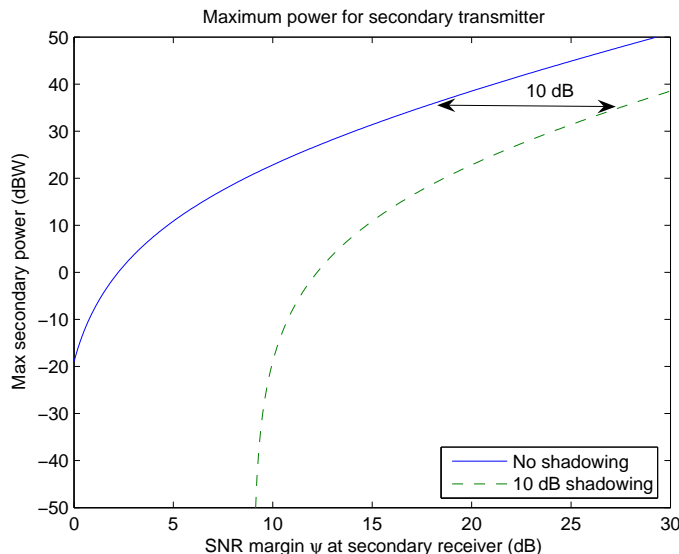


Fig. 27. Secondary users must assume that their received primary signal is attenuated not solely because they are far away, but partially due to some shadowing/fading effect.



Fig. 28. The probability of missed detection can be conditioned on the depth of the fade encountered. We are going to miss the signal for sure in the bad fades, even if we catch it perfectly when the fading is not so bad.

### H. Duty Cycle

For an 802.11b primary signal (minimum decodable SNR of 4 dB), with a 30 dB margin for protection and fading, a  $P_{MD} = 0.01$  can be achieved after sampling for a few tenths of a millisecond. Since a packet lasts a few milliseconds, these gaps may be exploitable if the secondary system is able to keep its dwell time (including all associated processing, cooperation, etc.) substantially shorter than the gaps in question.

When the target sensitivity is too low to allow the dwell time to lie well within a primary's on-time, then duty cycles make the problem harder since the secondary user is forced to listen for an amount of time spanning several packets without knowing when the packets are present.

Detecting a transmitter signal with only a 10% duty cycle is like detecting that signal with a 10 dB fade, with reference to its full strength. Such situations also block coherent processing since it is unlikely that pilots will remain coherent across primary packets.

Uncertainty in the duty cycle also further complicates matters. Assume that the primary system has agreed to accept a 1% probability of harmful interference. To guarantee this, we must be capable of detecting a signal's presence during its sparsest 1% of non-empty duty cycles. The duty cycle of a wireless link depends on the type of traffic, but traffic can vary in an unpredictable manner. Even if the current application is known, how to model the 1% sparsest packet transmissions is still an open question. A Poisson model "grievously underestimates the burstiness of TELNET traffic" [41]. In fact, empirical data from telnet traffic shows that over 15% of packet interarrival times were more than 1 second apart, and multiplexing does little to reduce the heavy tail of the distribution [41]. Without cooperation, it is impossible to be robust to uncertainty in fading and duty-cycle.

#### IV. COOPERATION AMONG COGNITIVE RADIOS

The previous section revealed that without cooperation, a cognitive radio needs a robust model of the 1% least-likely fades. This is essentially impossible in practice for any mobile device. Even with a model, Figure 29 plots the Complementary Cumulative Distribution Function (CCDF) of fading losses incurred by a radio. It is worth noting that for  $P_{MD} = 0.01\%$  (corresponding to secondary use with the footprints of at most  $K = 100$  non-cooperating users intersecting and a 1% probability of harmful interference) probability of detection we need to detect signals which are 56dB below the distance dependent path loss. Such sensitivities can impose very long integration times and furthermore, in Section II we have seen that in the presence of noise uncertainty, radios below the  $SNR_{wall}$  cannot improve their performance even with infinite integration time. Hence an single radio may be unable to perform robust sensing.

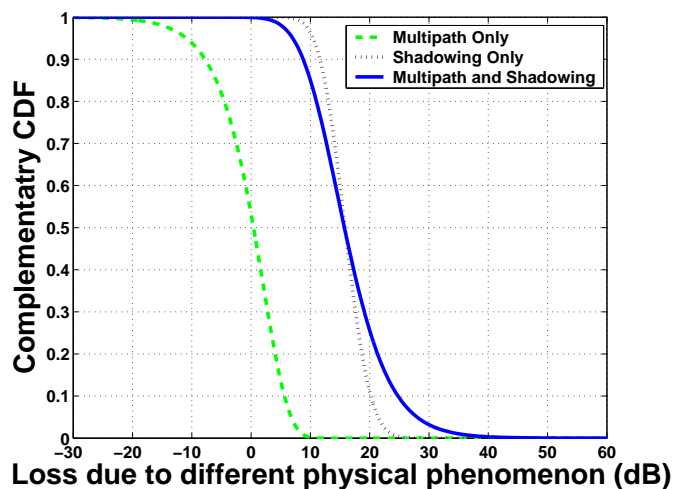


Fig. 29. Complementary CDF of Loss (in dB) due to different physical effects. Here we used a model of shadowing where shadowing is viewed as losses via a series of obstacles. For each obstacle, there is a small probability that the obstacle will be missed. Using this model, shadowing is viewed as *extra* loss beyond the distance dependent path loss. Mathematically, the net shadowing  $S$  can be expressed as  $S = \frac{1}{\sqrt{M}} \sum_{i=1}^M Y_i$  where  $Y_i$  is a random variable denoting the loss through a single obstacle.  $Y_i$  is  $\text{unif}(0, x)$  dB with probability 0.8 and zero otherwise. The loss per obstacle was adjusted to fit the variance of the measured log-normal standard variable of around 3.5dB [42]. The resulting value of  $M$  (number of obstacles encountered) was 15 while  $x$  was 10.25dB.

Putting duty-cycle issues<sup>14</sup> aside, there are two major sources of degraded signals. Multipath varies significantly with a displacement of  $\frac{\lambda}{4}$  as discussed in [29] (where  $\lambda$  is the wavelength). Shadowing on the other hand varies at the scale of 500m [43]. Since radio displacement is limited, multiple radios can act as a proxy. Specifically, if  $P_{D,system}$  is the overall probability of detection that the system must ensure, then the probability of detection of a single radio within the group ( $P_{D,radio}$ ) is  $1 - \sqrt[N]{1 - \frac{P_{HI}}{K}}$ , where  $N$  is the number of cooperating radios in the system and  $K$  is the number of noncooperating systems in the same area.

Cooperative gains is the improvement in sensitivity requirements once cooperation is employed (See Figure 30). Thus the device designer can figure out the implications of cooperation on the device specification through the well understood metric of detection sensitivity, thereby isolating the issue from unrelated concerns like the access regime.

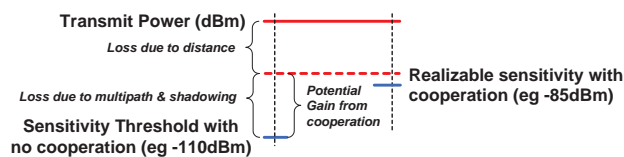


Fig. 30. Cooperation allows us to mitigate the effects of multipath and shadowing and hence the sensitivity threshold of a radio can be set closer to the value of nominal path loss. Gains from Cooperation are needed to overcome noise uncertainty limits and can further be used to decrease dwell times of the radios.

### A. Cooperative Regimes

The level of cooperation is determined by the bandwidth of the control channel and the quality of the detector. Using these two metrics we can define three regimes of interest:

- 1) **Low bandwidth control channel, Energy detector radios:** In this regime, we expect a low bandwidth control channel which is especially true of initial setup stages. Under such a scenario, it is realistic to assume that the radios exchange decisions or summary

<sup>14</sup>Cooperation helps in the context of low primary duty cycle when it can reject fading enough to get the required individual radio dwell times to be within the on-time or primary packet-lengths. What it can not do is reject the uncertainty in the duty-cycle itself since the realization of this is experienced in common by all the radios in the network since they are simultaneously facing the same primary.

statistics rather than long vectors of raw data. Furthermore, we assume radios that have no prior information about the correlation structure of the signal and hence must integrate the received energy. In Section II, we have seen that in the presence of noise uncertainty, energy detectors cannot detect a signal below a certain SNR value ( $SNR_{wall}$ ).

- 2) **Low bandwidth control channel, Detectors utilizing signal statistics:** An example of such detectors are cyclo-stationary detectors which utilize the correlation in the signal and hence perform better than energy detectors [44]. However, given the presence of a low bandwidth control channel, only summary statistics can be exchanged.
- 3) **High Bandwidth Control channel, All possible detectors:** In this regime, Cognitive Radios can exchange entire raw data and hence sophisticated detection can be performed. In this scenario, it may be possible for tightly synchronized radios to collectively overcome the  $SNR_{wall}$ .

The cooperation regime envisioned in this paper is the first regime described above which relies on a very low bandwidth, low latency, and long range control channel.

### B. Gains from Cooperation

Figure 31 shows the change in threshold with increasing number of users under three different effects: multipath only, shadowing only and multipath together with shadowing. We consider gains beyond the nominal path loss (as predicted by the multipath only curves) as artificial and these should be ignored. While gains increase with increased user participation, they asymptotically approach the nominal path loss.

### C. Soft versus Hard cooperation

It has been often argued that soft decision combining of sensing results yields gains which are much better than hard decision combining [46]. This is true when radios are tightly synchronized in which case they can collectively overcome the  $SNR_{wall}$  when the noise is independent at the different radios. If common interference is present along with the common primary, then an  $SNR_{wall}$  wall will again emerge and the effect of perfectly synchronized soft cooperation will only be to better reject uncorrelated interference sources, as well as to increase the number of samples available for averaging.

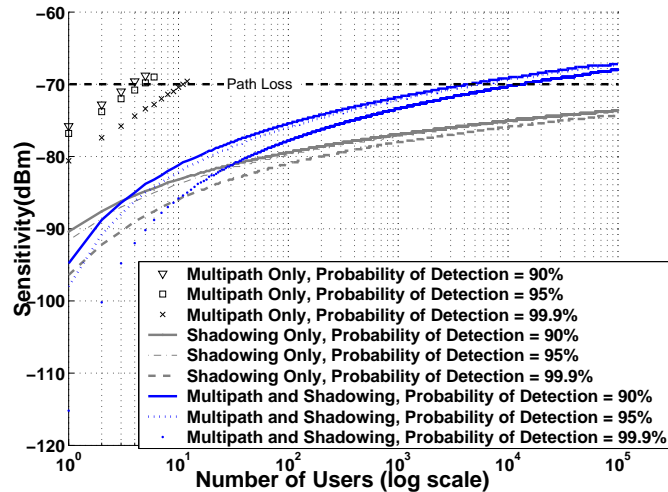


Fig. 31. Sensitivity variation with number of users (Frequency = 800MHz, Distance=60km, TV transmitter height=200m, CR height=3m). This simulation assumes path loss predictions by the NTIA model at a confidence level of 15% as the nominal distance dependent path loss [45]. This model accounts for losses due to frequency, distance, antenna heights, polarization, surface refractivity, electrical ground constants and climate and hence yields realistic loss levels. Each user performs a hard decision and sends the result to a central controller. With multipath only, results show an unbounded improvement in threshold as the number of users is increased. Multipath together with shadowing causes the threshold to asymptotically approach the nominal path loss. Half the gain is achieved by using 10 users, beyond which the gains exhibit ‘the law of diminishing returns’ as the number of users is increased.

To understand this better, consider the problem of detecting a signal in additive white Gaussian noise (AWGN) with an noise uncertainty  $\alpha$  (See Section II). For user  $i$ , our goal is to distinguish between the hypotheses:

$$\mathcal{H}_0 : Y_i[n] = \alpha W_i[n] \quad n = 1, \dots, M$$

$$\mathcal{H}_s : Y_i[n] = X[n] + \alpha W_i[n] \quad n = 1, \dots, M$$

Given that we are using a simple energy detector, the test statistics available under  $\mathcal{H}_0$  is [24]:

$$\mathcal{T}(Y_i) = \frac{1}{M} \sum_{j=1}^M \alpha^2 W_i[n]^2 \quad (43)$$

Its can be shown that:

$$\frac{MT(Y_i)}{\alpha^2 \sigma_w^2} \sim \chi_M^2 \quad (44)$$

For large  $M$ , this behaves as  $\mathcal{N}(M, 2M)$ . Hence we can approximate  $\mathcal{T}(Y_i)$  as  $\mathcal{N}(\alpha^2\sigma_w^2, \frac{2\alpha^4\sigma_w^4}{M})$ .

If we wish to have a net probability of false alarm ( $P_{FA}$ ) to be around 0.14 percent, the threshold should be set 3 standard deviations away from the mean. This places the threshold<sup>15</sup> at:  $\alpha_{max}^2\sigma_w^2(1 + \frac{\sqrt{2(9+\ln N)}}{\sqrt{M}})$ . The factor  $\alpha_{max}^2\sigma_w^2$  is the worst case noise power.

For soft decoding, we can bound performance by assuming that all the samples are provided to the user with the best channel. In that case the probability of false alarm threshold can be set at:  $\alpha_{max}^2\sigma_w^2(1 + \frac{3\sqrt{2}}{\sqrt{MN}})$ , where  $N$  is the number of users.

To observe the differences between soft and hard decoding we simulated a group of users at a distance of 60km from the TV transmitter. The number of users in this group was varied and the effect on radio sensitivity for a 95% probability of detection was observed. The results of this simulation can be seen in Figure 32. The small difference between hard and soft decision arises from the larger number of samples available in the soft case. But unless the primary duty cycle is the key constraint, the  $SNR_{wall}$  due to uncertainty is a bigger constraint than the limitation in the dwell time.

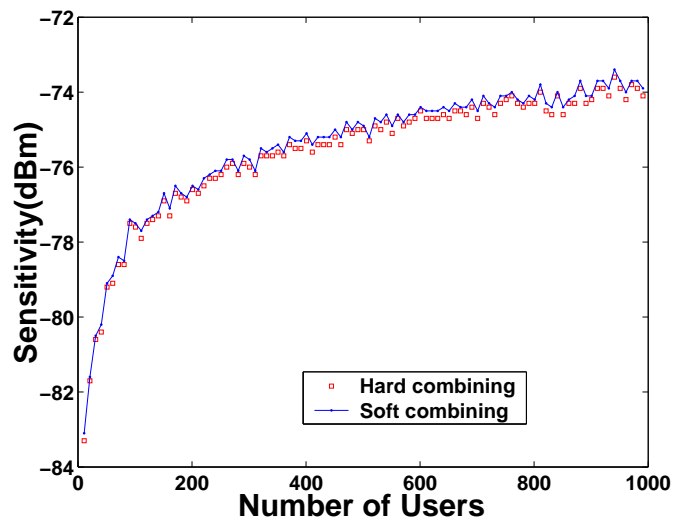


Fig. 32. Radio sensitivity for soft versus hard decoding. The difference between soft and hard decoding is due to the effect of finite number of samples

<sup>15</sup>We need to introduce the tiny  $\sqrt{\log N}$  correction term to translate system-level false alarm probabilities to radio-level false alarm probabilities.

### D. Shadowing Correlation

Shadowing exhibits high correlation if two radios are blocked by the same obstacle. Shadowing correlation displays distance dependence which has been studied extensively [43]. In [43] an exponential model is proposed to fit the measured data. To better understand the exponential trend, we constructed a model where two radios separated by a distance  $D$  are blocked from the primary transmitter by a layer of obstacles (See Figure 33). Each layer consists of buildings interspersed by empty spaces. This model fits better than the exponential model proposed in [43] (See Figure 33).

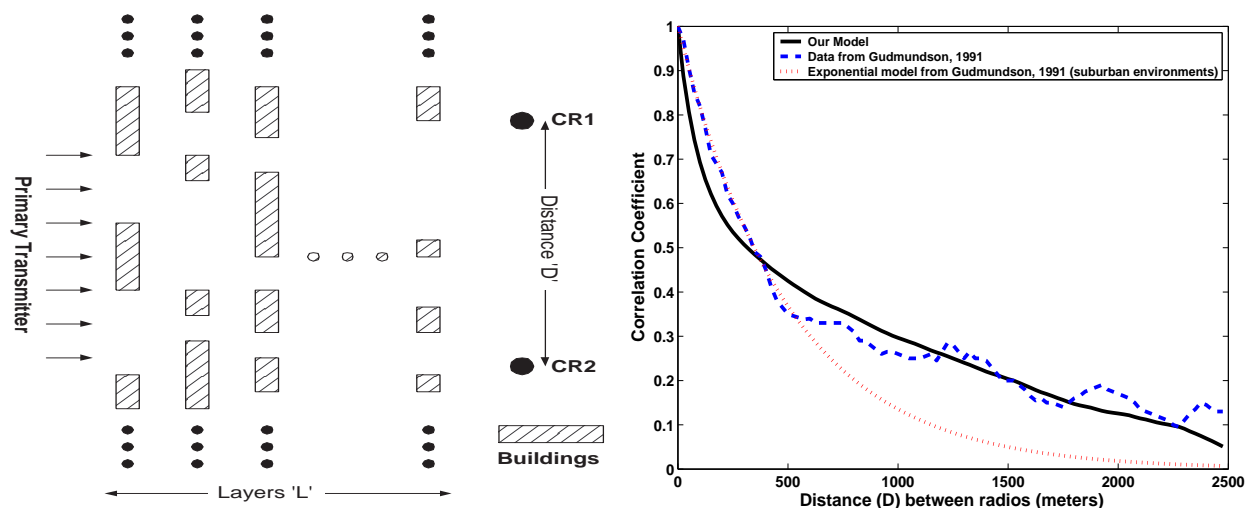


Fig. 33. Model of shadowing correlation derived by considering the loss correlations between  $CR_1$  and  $CR_2$  which are separated by a distance  $D$ . The radios are separated from the primary transmitter via a finite layer ( $L$ ) of obstacles. Each layer consists of buildings interspersed with free space. Building length is exponentially distributed with mean  $\mu_{building}$  while the free space length is exponentially distributed with mean  $\mu_{space}$ . The parameters that best fit the data in [43] are the following:  $\mu_{building} = 100m$ ,  $\mu_{space} = 1000m$ ,  $L = 4$ . This model fits better than the exponential model proposed in [43]

To study the effect of shadowing correlation, we simulated a group of cognitive users in a line at a distance of 60km from a TV transmitter as shown in Figure 34. The polling entity located at the center of this group examines the detection results of users. The effect of increasing users on the sensitivity threshold of an individual radio can be seen in Figure 35. All forms of correlation (constant or distance dependent) only serve to increase the number of users required to achieve a given sensitivity reduction. Increased correlation decreases our chances of getting a user with a very good channel and hence more users need to be polled for independent looks at the same random variable. For distance dependent correlation, this translates into a desire to poll

users which are further away.<sup>16</sup> This effect can be seen in Figure 36. Here, we are interested in studying how the required sensitivity varies with the number of users and their distance spread. Increasing the number of users for a given distance spread asymptotically reaches a limit which is dependent on the distance spread. It is reasonable to call this distance spread the *cooperative footprint* of the cognitive network.

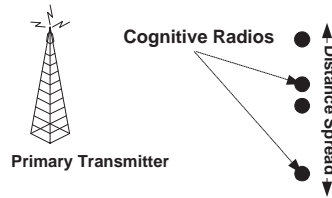


Fig. 34. Simulation setup for distance dependent shadowing correlation.

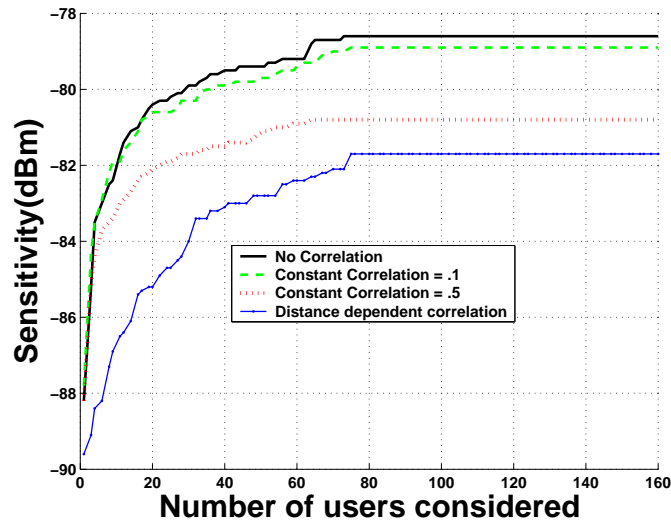


Fig. 35. Sensitivity variation with number of users under different correlation characteristics (no multipath). Correlation causes the system to poll more users to achieve a given threshold. For distance dependent correlation we choose a linear increase model since the shadowing correlation model developed earlier as well as the exponential model proposed in [43] only predict one dimensional correlation.

<sup>16</sup>Of course, the users should also be close enough to be seeing the same primary user. This suggests that cooperative gain will be hard to achieve for primary users with very small footprints.

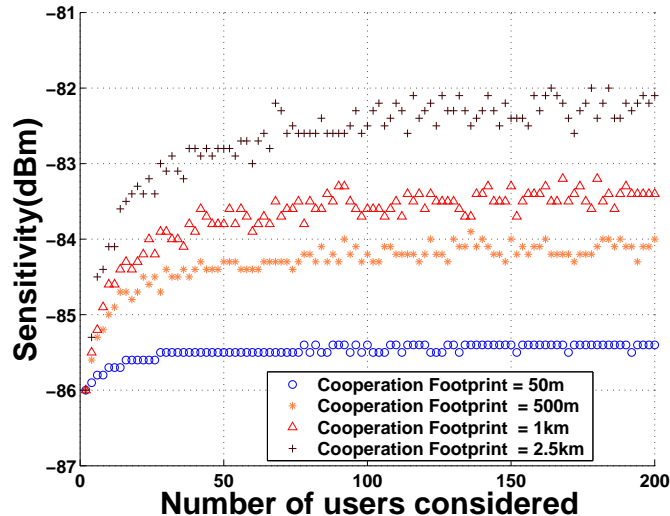


Fig. 36. Comparing the impact of varying users versus varying the distance spread. Each set of points represents increased user density. Increasing the number of users for a given distance spread asymptotically reaches a limit which is dependent on the distance spread. A similar effect can be seen in [46] where the probability of missed opportunity does not go to zero in a correlated environment. The plot emphasizes the need for independent samples; gains from increasing the number of users is asymptotically limited in a correlated environment.

### E. Impact of Untrusted/Unmodeled Users

For cooperative sensing, trust issues arise naturally given the usage model. Sensing a frequency band consumes energy and time which may have been better used for data transmission. Hence users have an incentive to either not sense at all or to sense for a shorter duration than stipulated. Furthermore, for an individual user, there may be a valid reason to report detection results in a certain way. They can either assert the presence of a primary user, in which case they deny others the opportunity to take advantage of the available bandwidth, or always deny the presence of primary users. Uncertainty in user behavior impacts cooperative gains in a significant way.

Figure 37 shows the impact of having a fraction  $\alpha$  of  $N$  users behave unpredictably (this fraction may swing between reporting presence of the primary and its absence in a random fashion). To cater for the case when this fraction always reports the presence of a primary, we can set the detection threshold at  $\beta N$  where  $\beta > \alpha$  ie. we declare that a primary user is present only if  $\beta N$  cognitive radios see the primary user. The problem arises when these radios start reporting the absence of a primary user. Not only do they effectively reduce the number of real users in the system to  $N(1 - \alpha)$ , but they also now require a fraction  $\frac{\beta}{1-\alpha}$  of the trustworthy

users to detect the signal. Explicitly, the resulting probability of detection for a given threshold  $t$  is given by:

$$P_{d,t} = 1 - \sum_{i=0}^{\beta N - 1} \binom{N(1-\alpha)}{i} (1 - F(t))^i F(t)^{N(1-\alpha) - i} \quad (45)$$

where  $F(t)$  is the cdf of the received signal strength.

From Figure 37, we see that the individual sensitivity threshold tolerable for a group with a fraction of  $\alpha$  untrusted users is roughly the same as that achievable by a trusted system with  $\frac{1}{\alpha}$  users. The intuition is that when the number of independent users is large, for a fraction  $\frac{\beta}{1-\alpha}$  of them to detect the primary requires that the threshold be set low enough so that  $F(t) \leq 1 - \frac{\gamma\beta}{1-\alpha}$  where  $\gamma$  is a function of  $P_{MD}$ .

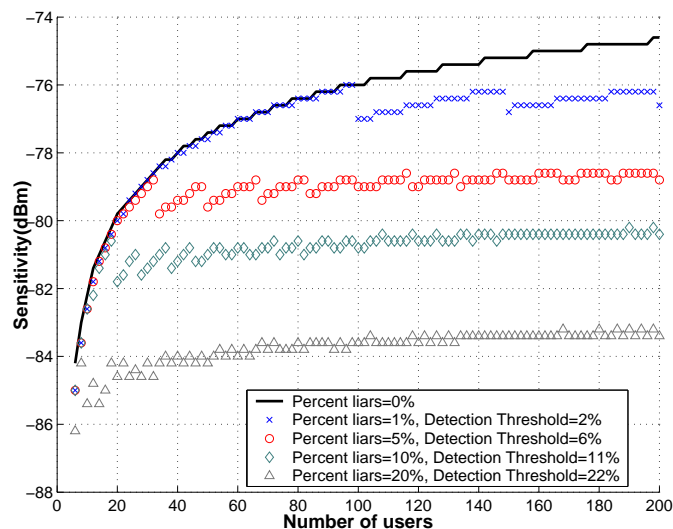


Fig. 37. Sensitivity Variation with malicious adversaries. The individual sensitivity threshold tolerable for a group with a fraction of  $\frac{1}{N}$  liars is the same as that achievable by a trusted system with  $N$  users. This threshold forms an upper bound even when the actual number of users is increased beyond  $N$ . Hence for 1% liars, the final achievable threshold is -76dBm which is the threshold for a trusted system with 100 users. It must be noted that these gains are asymptotically achievable for large  $N$  especially for a large percentage of malicious users.

## V. FAIRNESS AND THE NEED FOR LOCAL COOPERATION

The uncertainty due to fading can be tamed with a trustworthy cognitive network with a large cooperative footprint. However, the uncertainty due to the nearby secondary users remains. The radiometer cannot distinguish between the primary signal and transmissions from secondary users. This is a fairness issue since secondaries should be equal in priority and the first secondary to use a band should not be able to capture it for his exclusive use. An individual node or even a cooperating network has no way of knowing whether it is alone or surrounded by other active secondaries. Secondary interference could thus range from a minimum of zero to a maximum density determined by the power control law. Cooperation with a distant radio does not impact this uncertainty since it acts at the level of the individual radio's noise, not at the level of primary signal attenuation.

To robustly detect a weak primary signal in a fair manner, this uncertainty must be reduced. We propose the “sensing MAC” form of local cooperation: systems within a certain “shut-up” radius  $r_s$  of the sensing node must remain quiet for the duration of sensing. The tradeoff between the sensing radius and the secondary power density is developed in the next section.

### A. Power/Cooperation tradeoffs: non-coherent case

To arrive at the required power-cooperation tradeoff, we first start with a given secondary power density  $D$ . This power density induces a maximum possible aggregate interference,  $I_{aggregate}(r)$  at the primary receivers located at a distance of  $r$  from the primary transmitter. We must ensure that all primary receivers within the protected radius are still able to decode their primary transmissions. Under this constraint it is possible to calculate a lower bound on the no-talk radius:  $r_n \geq r_p + \left[ \frac{K(\alpha_{21})D}{(10^{\frac{\beta}{10}} - 1)\sigma^2} \right]^{\frac{1}{\alpha_{21}-2}}$ . The sensors at the edge of the no-talk radius  $r_n$  receive a primary signal of power  $P_n = P_{primary} r_n^{-\alpha_{12}} 10^{\frac{\beta}{10}}$ . Here we account for  $\beta$  dB of possible fading and duty-cycle thinning, counting on long-distance cooperation within the cognitive network to take care of the rest. For the radio to be able to detect the primary signal,  $P_n$  must be greater than the uncertainty in the noise plus interference. The uncertainty at the sensor can be divided into two categories: device level uncertainty and uncertainty due to other secondary transmissions. The device level uncertainty can be accounted for by assuming that the noise variance lies in  $[\frac{1}{\rho}\sigma^2, \rho\sigma^2]$  for some suitable  $\rho \geq 1$ . Since we do not know the number of actual interferers, the total interference can lie anywhere in  $[0, I_{max}]$ , where  $I_{max} = D \frac{2\pi}{\alpha_{22}-2} r_s^{-\alpha_{22}+2}$  is the maximum possible interference from secondaries outside the shut-up radius  $r_s$ . Therefore, the actual noise plus interference can lie in  $[\frac{1}{\rho}\sigma^2, \rho\sigma^2 + I_{max}]$ . So in order to overcome the SNR wall we must

have  $P_n \geq I_{max} + \frac{\rho^2-1}{\rho}$ . Hence we get the required tradeoff between  $D$  and  $r_s$ :

$$r_s \geq \left[ \frac{D \left( \frac{2\pi}{\alpha_{22}^2-2} \right)}{P_n - \frac{\alpha^2-1}{\alpha}} \right]^{\frac{1}{\alpha_{22}^2-2}} \quad (46)$$

Figure 38 plots the power-cooperation tradeoff for different values of fading margins and power decay models. This clearly shows that the required coordination radius is unreasonably high under radiometric detection even after long-distance cooperation. Since the MAC protocols for data traffic are usually energy detector based, this indirectly tells us that the data MAC is not going to be good enough to perform the role for sensing. In order to reduce the sensing MAC shut-up radius  $r_s$ , it is clear that we need to estimate the interference from the secondary transmissions (see section II-F). Figure 39 shows the new power-cooperation tradeoff using the gains from interference estimation. It is clear that  $r_s$  is still impractically large.

### B. Power/Cooperation tradeoffs: coherent case

Now, we re-derive the power-cooperation tradeoff given in (46) for the coherent detector also taking into account in-band interference estimation. Let  $\lambda$  denote the percent interference estimation error (see Figure 17). The new tradeoff is given by

$$r_s \geq \left[ \frac{D \left( \frac{2\pi}{\alpha_{22}^2-2} \right) \lambda}{z\theta P_n - \frac{\alpha^2-1}{\alpha}} \right]^{\frac{1}{\alpha_{22}^2-2}} \quad (47)$$

where  $z$  is the coherent processing gain. The above tradeoff is very similar to the one in (46). The  $\lambda$  in the numerator is because the uncertainty in the interference is reduced from  $I_{max}$  to  $\lambda I_{max}$ . Also, the effective signal power at the no-talk region is  $z\theta P_n$  because the sensors try to detect the primary pilot tone and the pilot strength is boosted due to coherent signal processing within each channel coherence block. Figure 41 shows the power-cooperation tradeoff with coherent processing gains included.

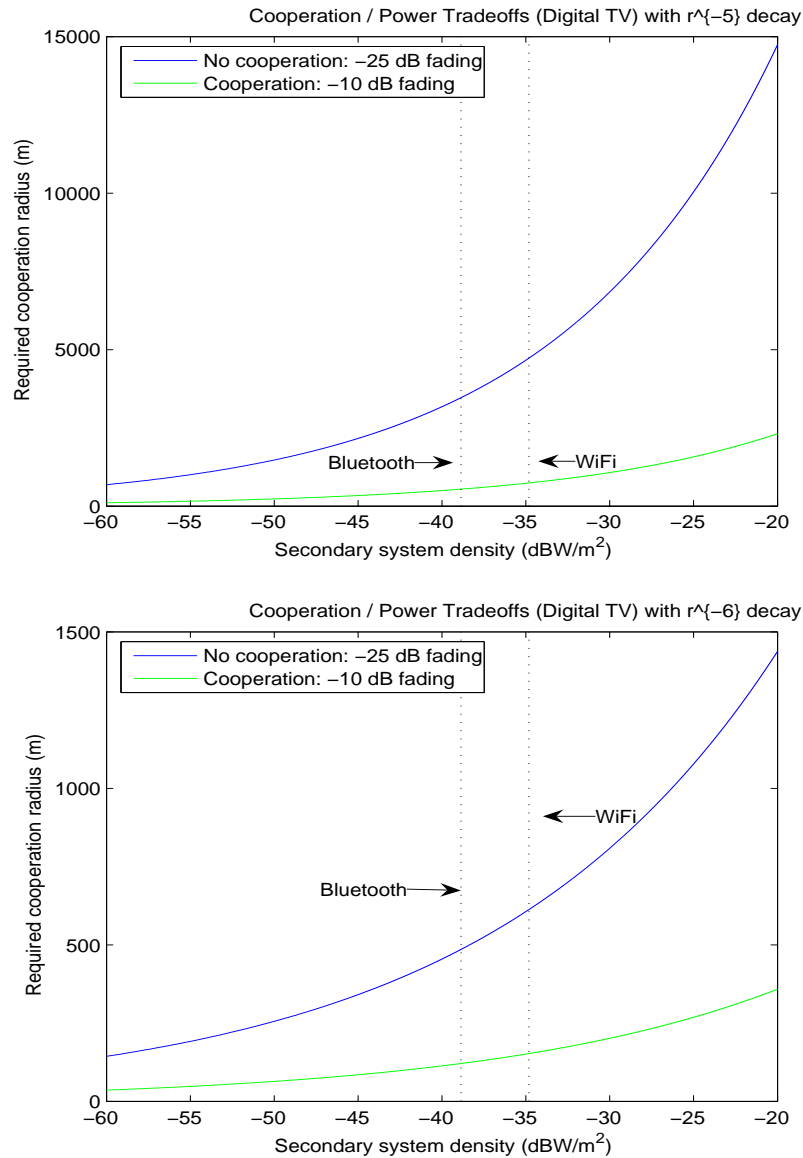


Fig. 38. The cooperation radius  $r_s$  is plotted as a function of the secondary power density for opportunistic use within the digital TV bands. The figure on the top has been plotted using an  $r^{-5}$  power decay rule for secondary transmissions. The two curves in this figure correspond to 25 dB and 10 dB fading margins. The dotted vertical lines correspond to a transmit power of 2.4 mW over a radius of 2.5 m for Bluetooth and 100 mW over a radius of 10m for 802.11b. This figure clearly illustrates that within system cooperation is essential to mitigate the effect of fading. Also, the cooperation radius  $r_s$  is of the order of hundreds of meters or a few kilometers, which is ridiculously high even for reasonable power density levels. The figure on the bottom shows the same tradeoff assuming that the secondary power decays as  $r^{-6}$  with distance. It is immediately apparent that there is a decrease in the required cooperation radius  $r_s$  for the same power density. This shows that the power-coordination tradeoff obtained is very sensitive to assumptions on the power decay models. However, in both models the required coordination radius is unreasonably high.

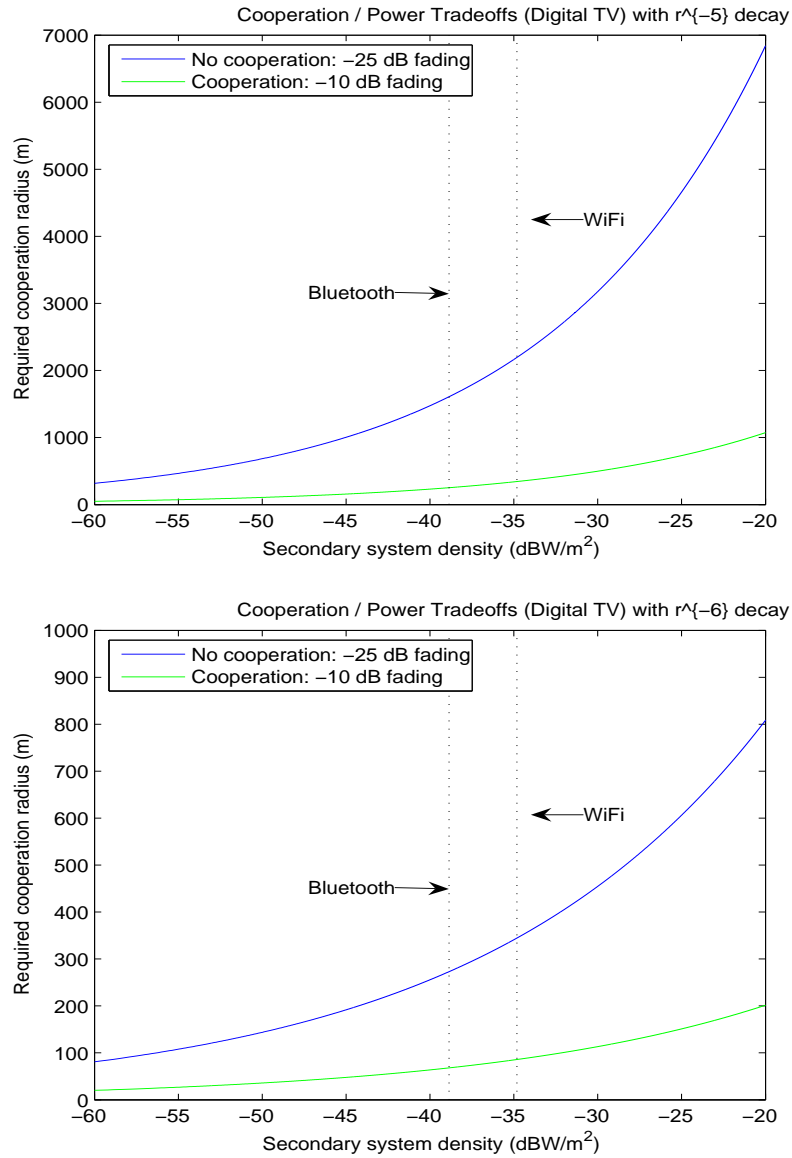


Fig. 39. The cooperation radius  $r_s$  is plotted as a function of the secondary power density. The top plot corresponds to a secondary power decay of  $r^{-5}$  and the bottom one corresponds to a secondary power decay of  $r^{-6}$ . Here we assume that the interference estimation error is 10%.

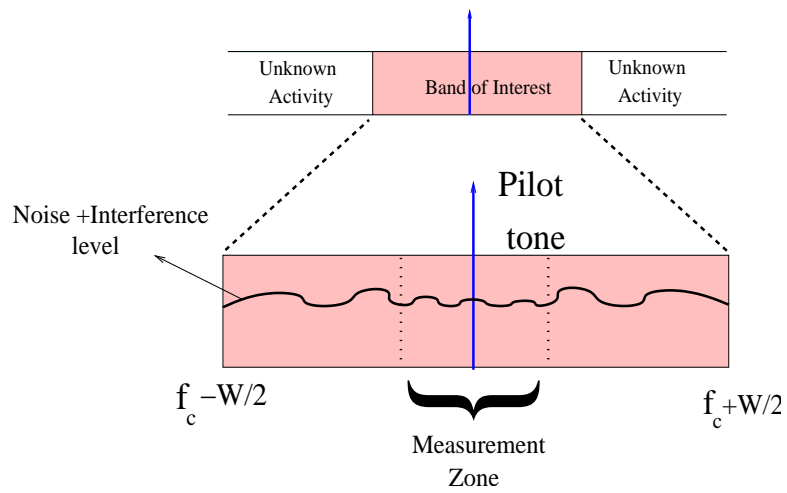


Fig. 40. In band interference estimation. As the bandwidth of the pilot is considerably smaller than the whole band, we can estimate the interference by taking measurements close to the pilot frequency. This reduces the interference estimation error.

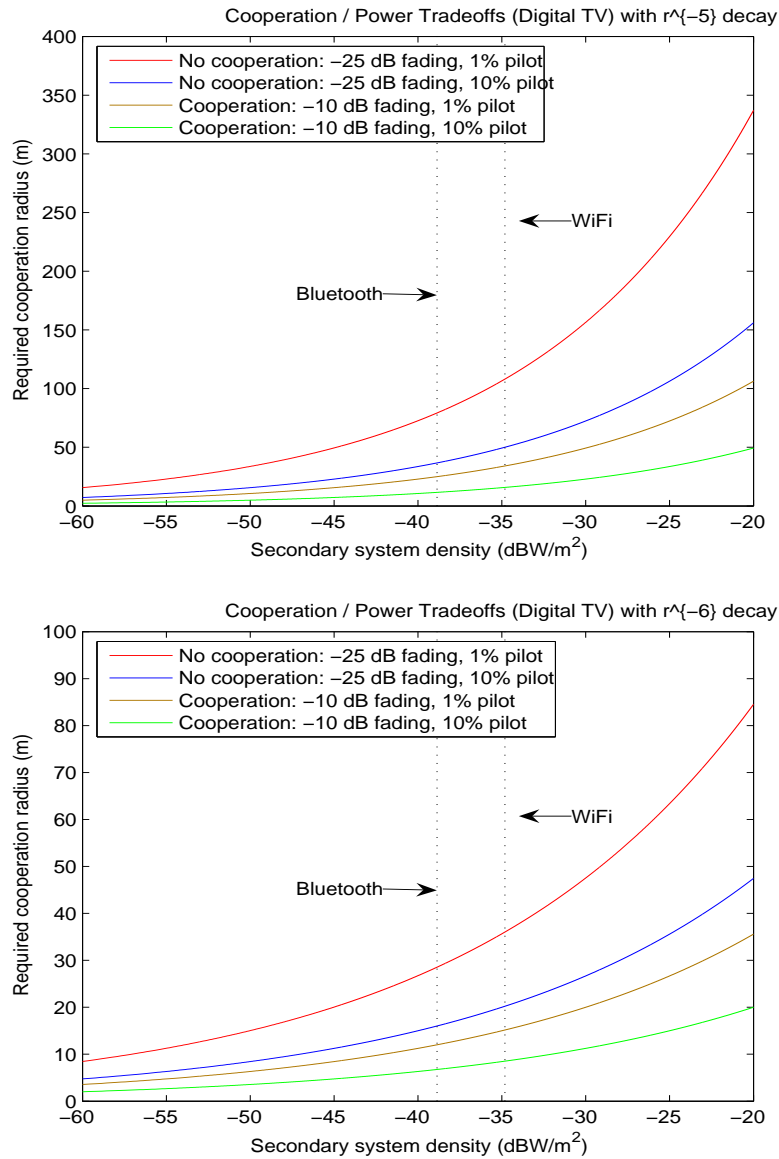


Fig. 41. The cooperation radius  $r_s$  is plotted as a function of the secondary power density. Each plot contains curves corresponding to 1% and 10% pilot energy. The top plot corresponds to a secondary power decay of  $r^{-5}$  and the bottom one corresponds to a secondary power decay of  $r^{-6}$ . Here we assume that the interference estimation error is 1%. It is clear that the amount of cooperation required is within 100 meters when we have to account for only 10 dB of shadowing margin. We compare tradeoff curves for 10 dB shadowing with those corresponding to 25 dB shadowing margin. This illustrates the fact that we cannot completely dispense of the need for intra-system cooperation.

## VI. EXPONENTIAL PATH LOSSES

Polynomial decay functions are poor models for attenuation in cluttered, urban environments. A decay function of the form  $g(r) = r^{-\alpha} \cdot e^{-\lambda r}$  more accurately models the effects of absorption and multipath for far away receivers [36]. In this section we examine the effects of using this more representative model.

### A. Effects of the exponential attenuation model

With an polynomial attenuation model, we modeled a system's non-shadowing/multipath path loss as polynomial decay with a fairly high exponent (i.e.  $r^{-3.5}$ ,  $r^{-5}$ ). If we use  $r^{-\alpha} \cdot e^{-\lambda r}$ , the  $\alpha$  will be smaller to compensate for the exponential component. In other words, the signal is better described by saying it is stronger closer to the transmitter and weaker further away than our polynomial model would otherwise indicate.

This effect has several implications. First, assume that the no-talk radius is fairly close to the protected radius. The aggregate interference to a primary receiver on the protected radius then decays nearly polynomially, but more slowly than in our previous model. Thus, the physical margin of protection  $r_n - r_p$  must be significantly larger.

Furthermore, since its protected radius is so large, the primary signal will likely be decaying nearly exponentially by the protected radius. The signal will continue to attenuate rapidly out to the no-talk radius, at which point it will be extremely weak.

Detecting these weak signals will be much more difficult than under the polynomial model. The fairness requirement will also be far more restrictive. The shutup radius must now be large enough that the aggregate interference at a secondary transmitter is weaker than the now very weak primary signal. Again, this aggregate interference will be decaying nearly polynomially, so the shutup radius will be impractically large, or the low-powered secondary nodes must be placed very sparsely.

### B. Implications

The requirement of a large shutup radius stems largely from the asymmetry in the secondary signal's attenuation versus the primary signal's attenuation between the protected radius and the notalk radius.

This effect can be diminished by reducing the distance between the protected radius and the notalk radius. This counterintuitive result tells us that inefficient policymaking - allowing an excessive margin of protection to the primary system - actually has serious adverse effects on opportunistic systems, beyond wasted geographic area. On the topic of wasted geographic area, it is worth mentioning that if signals are decaying exponentially, the lost geographic area from shadowing uncertainty is diminished, because shifting the notalk radius outward by, say, 30 dB covers a much smaller region.

Attenuation asymmetry is also reduced if the secondary signal attenuation fairly near the secondary transmitters occurs roughly at the same rate as the primary signal attenuation far from the transmitters. In other words, opportunistic devices will interact far more successfully with primaries if the opportunistic devices combat ground bounces and indoor environments than if they mount antennas on tall towers or buildings.

### C. Numeric examples

We denote the path loss from, say, the primary transmitters to a secondary system as  $g_{12}(r) = r^{-\alpha_{12}} \cdot e^{-\lambda_{12}r}$ . For simplicity, we continue to assume  $g_{11}(r) = g_{12}(r)$ . We also use the straight-line approximation for the secondary interference because of the limitations of the numeric solver. We are lower bounding the interference, so the numeric results below must be taken with a grain of salt; however, the bound is reasonably tight. We address three cases:

- $\alpha_{11} = \alpha_{21}$ ,  $\lambda_{11} = \lambda_{21}$  In this case the the secondary transmit antennas and the primary transmit antennas are approximately the same height.

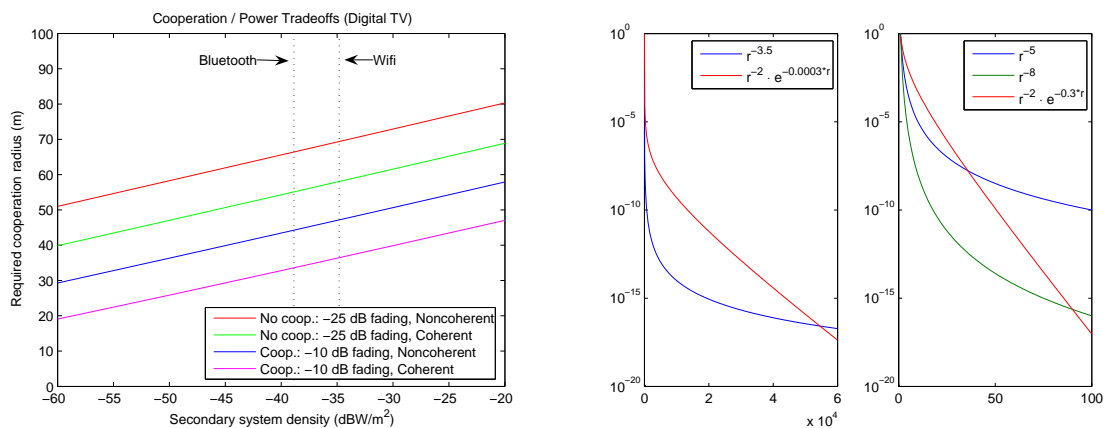
We pick  $g_{11}(r) = r^{-2} \cdot e^{-0.0003r}$  as the decay function because there is a 166 dB loss over 55 km, putting the limit of decodability for digital TV near the Grade B contour. With a protection margin of 10 dB, the protected radius is about 47 km. The no-talk radius, however, is another 41 km further out! Even ignoring fading, a cognitive radio at that distance is forced to detect a -164 dB signal. Almost any uncertainty renders the signal completely undetectable. Opportunistic devices will fail under these constraints.

- $\alpha_{11} = \alpha_{21}$ ,  $\lambda_{11} < \lambda_{21}$  (Figures 42-44.)

If the secondary transmit antennas are closer to the ground (likely for low-powered opportunistic devices) they will experience more interference and absorption from ground bounces

and clutter in the environment. This will lead to a larger  $\alpha$  and  $\lambda$ . We consider these two cases separately.

Figure 42 shows the necessary shutup radius when the secondary signals experience rapid exponential attenuation. Figure 43 presents the same plot with less rapid secondary attenuation, and Figure 44 has even slower attenuation. In Figure 44 it is apparent that without coherent detection or cooperation, there is a fundamental limit on the density of secondary users.

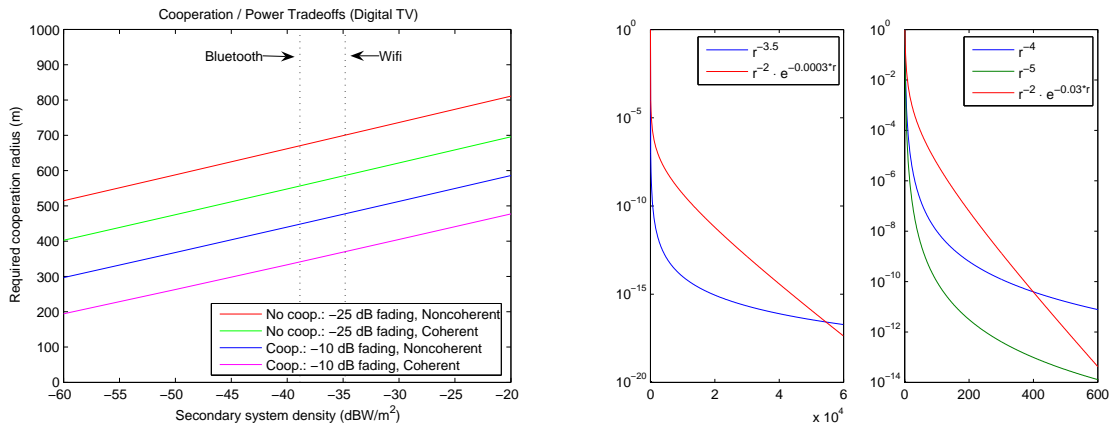


(a) Necessary shutup radius, within which intersystem co- (b) Comparison of exponential model with polynomial operation is required. models.

Fig. 42. We use  $g_{11}(r) = r^{-2} \cdot e^{-0.0003r}$  and a 10 dB margin of protection. Because of the exponential decay, larger margins of protection correspond to smaller physical distances. (a) shows the required shutup radius for if the secondary signals attenuate as  $g_{21}(r) = r^{-2} \cdot e^{-0.3r}$ . (b) compares  $g_{11}(r)$  and  $g_{21}(r)$  to polynomial decay functions across distances on the order of  $r_p$  and  $r_s$ , respectively.

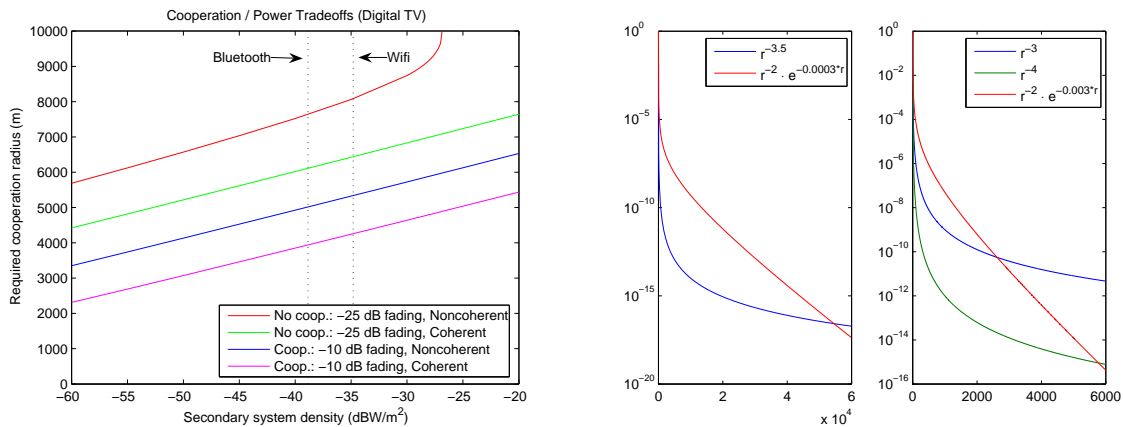
- $\alpha_{11} < \alpha_{21}$ ,  $\lambda_{11} = \lambda_{21}$  (Figure 45.)

If the exponential term  $\lambda$  is not large enough to have a significant effect over distances of the order of  $r_p - r_n$  Figure 45 is more similar to the graphs in Section V.



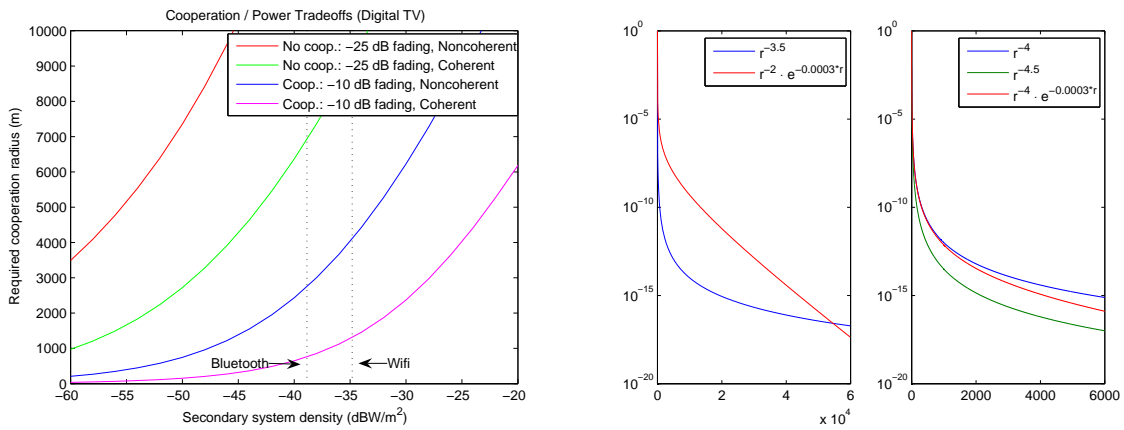
(a) Necessary shutup radius, within which intersystem co- (b) Comparison of exponential model with polynomial operation is required. models.

Fig. 43. We use  $g_{11}(r) = r^{-2} \cdot e^{-0.0003r}$  and a 10 dB margin of protection. Because of the exponential decay, larger margins of protection correspond to smaller physical distances. (a) shows the required shutup radius for if the secondary signals attenuate as  $g_{21}(r) = r^{-2} \cdot e^{-0.03r}$ . (b) compares  $g_{11}(r)$  and  $g_{21}(r)$  to polynomial decay functions across distances on the order of  $r_p$  and  $r_s$ , respectively.



(a) Necessary shutup radius, within which intersystem co- (b) Comparison of exponential model with polynomial operation is required. models.

Fig. 44. We use  $g_{11}(r) = r^{-2} \cdot e^{-0.0003r}$  and a 10 dB margin of protection. Because of the exponential decay, larger margins of protection correspond to smaller physical distances. (a) shows the required shutup radius for if the secondary signals attenuate as  $g_{21}(r) = r^{-2} \cdot e^{-0.003r}$ . (b) compares  $g_{11}(r)$  and  $g_{21}(r)$  to polynomial decay functions across distances on the order of  $r_p$  and  $r_s$ , respectively.



(a) Necessary shutup radius, within which intersystem co- (b) Comparison of exponential model with polynomial operation is required. models.

Fig. 45. We use  $g_{11}(r) = r^{-2} \cdot e^{-0.0003r}$  and a 10 dB margin of protection. Because of the exponential decay, larger margins of protection correspond to smaller physical distances. (a) shows the required shutup radius for if the secondary signals attenuate as  $g_{21}(r) = r^{-4} \cdot e^{-0.0003r}$ . (b) compares  $g_{11}(r)$  and  $g_{21}(r)$  to polynomial decay functions across distances on the order of  $r_p$  and  $r_s$ , respectively.

## VII. CONCLUSIONS

This paper explored the basic physical-layer induced limits on secondary use of the radio spectrum subject to the constraint of non-interference with the primary users. The uncertainties that are traditionally controlled using space and frequency guard bands must now be dealt with using dynamic signal processing and interactive protocols. Consequently, the limits on robust signal processing give rise to the fundamental limits here and prevent the detection of very weak signals. At the level of modeling, the challenging uncertainties come from the shadowing environment and the possibly varying duty-cycle of the primary user. Shadowing is independent when considered at a large enough physical scale. As a result, a secondary radio network can escape having to deal with exceptionally bad shadowing by ensuring that it has a geographically large enough cooperation footprint. Even so, the uncertainty in the trust/reliability of the nodes within the network imposes another bound on the cooperative gain achievable. Since the duty-cycle is common for all users, the only hope around this uncertainty is for the final dwell-times for sensing to be contained well within an on-period for the primary.

At a higher level, another major uncertainty comes from the interference produced by secondary users who are outside of our cooperating network. Those that are nearby will put a lot of energy into the band and risk confusing us into thinking that the primary user is active. This is fundamentally a fairness issue since that would allow secondary networks to deny others access to an empty band. To mitigate this uncertainty, users nearby must cooperate by not transmitting while the primary is transmitting. But to be practical, the sense of “nearby” must not be too large or coordination is going to be impossible.

As a result, it turns out that energy-detector based methods can not work robustly, even after long-distance cooperation in bands whose primary inhabitants are very strong television-type signals. While energy-detectors are good enough for data MAC protocols and to enforce local power density limits, some form of coherent detectors are required for sensing the primary in order to get processing gain and to be able to estimate and thereby suppress the impact of interference coming from far away unknown secondary users. To have an ad-hoc cognitive network function robustly, it seems that we require a combination of a large cooperative footprint in a relatively well trusted network, a sensing-MAC among possibly non-cooperative users nearby, and coherent signal processing with interference estimation within the individual nodes.

Cooperation is just another word for infrastructure and so the need for all this cooperation for robust operation even in the relatively simple TV bands suggests that opportunistic use beyond the UWB-style will require some infrastructure in general. The difference between the various modes of secondary use from Table I is likely to be in the type of infrastructure that they need. One advantage of opportunistic use is that it does seem possible to deploy the infrastructure in stages without requiring the explicit assent of primary users.

As the discussion of hard vs. soft cooperation indicates, the cooperating infrastructure can be relatively lightweight in its data needs. This suggests that sensing to enable opportunistic use may become a gateway to the evolution of competitive band-managers. Band-managers can specialize in sensing and herd cognitive users without needing to “own” bands themselves. The price they can charge will be determined by the relative complexity reductions that they can enable at the user nodes rather than the congestion in the wireless spectrum. Once the spectral gaps begin to become filled, pricing to control congestion is likely to be needed, and will likely happen as band-managers try to acquire primary rights to various bands in order to guarantee QoS to their customers.

## REFERENCES

- [1] NTIA, "US frequency allocation chart," 2003. [Online]. Available: <http://www.ntia.doc.gov/osmhome/allochrt.html>
- [2] R. W. Broderson, A. Wolisz, D. Cabric, S. M. Mishra, and D. Willkomm, "White paper: CORVUS: A Cognitive Radio Approach for Usage of Virtual Unlicensed Spectrum," Tech. Rep., 2004. [Online]. Available: [http://bwrc.eecs.berkeley.edu/Research/MCMA/CR\\_White\\_paper\\_final1.pdf](http://bwrc.eecs.berkeley.edu/Research/MCMA/CR_White_paper_final1.pdf)
- [3] "Report of the Spectrum Efficiency Working Group," Federal Communications Commission, Tech. Rep. 02-135, Nov 2002. [Online]. Available: [www.fcc.gov/sptf/files/SEWGFfinalReport\\_1.pdf](http://www.fcc.gov/sptf/files/SEWGFfinalReport_1.pdf)
- [4] M. A. McHenry, "NSF spectrum occupancy measurements project summary," Shared Spectrum Company, Tech. Rep., Aug. 2005. [Online]. Available: [http://www.sharespectrum.com/inc/content/measurements/nsf/NSF\\_Project\\_Summary.pdf](http://www.sharespectrum.com/inc/content/measurements/nsf/NSF_Project_Summary.pdf)
- [5] FCC, "FCC 03-122," Tech. Rep., May 2003. [Online]. Available: [http://hraunfoss.fcc.gov/edocs\\_public/attachmatch/FCC-03-322A1.pdf](http://hraunfoss.fcc.gov/edocs_public/attachmatch/FCC-03-322A1.pdf)
- [6] I. J. Mitola, "Software radios: Survey, critical evaluation and future directions," *IEEE Aerosp. Electron. Syst. Mag.*, vol. 8, pp. 25–36, Apr. 1993.
- [7] Y. Benkler, "Overcoming agoraphobia: Building the commons of the digitally networked environment," *Harvard Journal of Law & Technology*, vol. 11, pp. 287–400, Winter 1998.
- [8] New America, et al., "Technical reply," Jan. 2005. [Online]. Available: [http://www.newamerica.net/Download\\_Docs/pdfs/Doc\\_File\\_2202\\_1.pdf](http://www.newamerica.net/Download_Docs/pdfs/Doc_File_2202_1.pdf)
- [9] R. Etkin, A. Parekh, and D. Tse, "Spectrum sharing for unlicensed bands," in *IEEE DySPAN 2005*, Baltimore, MD, Nov.8–11 2005.
- [10] A. S. de Vany, R. D. Eckert, C. J. Meyers, D. O'Hara, and R. Scott, "A property System for Market Allocation of the Electronic Spectrum: A Legal-Economic-Engineering Study," *Stanford Law Review*, vol. 21, pp. 1499–1561, June 1969.
- [11] D. N. Hatfield and P. J. Weiser, "Property Rights in Spectrum: Taking the Next Step," in *IEEE DySPAN 2005*, Baltimore, MD, Nov.8–11 2005, pp. 43–55.
- [12] G. Faulhaber and D. Farber, "Spectrum management: Property rights, markets, and the commons," in *Telecommunications Policy Research Conference Proceedings*, 2003.
- [13] E. Kwerel and J. Williams. (2002) A proposal for a rapid transition to market allocation of spectrum. [Online]. Available: [http://hraunfoss.fcc.gov/edocs\\_public/attachmatch/DOC-228552A1.pdf](http://hraunfoss.fcc.gov/edocs_public/attachmatch/DOC-228552A1.pdf)
- [14] J. Huang, R. Berry, and M. L. Honig, "Distributed interference compensation for wireless networks," 2006, to appear in special issue on "Price-based Access Control and Economics for Communication Networks".
- [15] O. Ileri, D. Samardzija, T. Sizer, and N. Mandayam, "Demand Response Pricing and Competitive Spectrum Allocation via a Spectrum Server," in *IEEE DySPAN 2005*, Baltimore, MD, Nov.8–11 2005, pp. 194–202.
- [16] FCC, "FCC 98-153," Sept. 1998. [Online]. Available: [http://www.fcc.gov/Bureaus/Engineering\\_Technology/Notices/1998/fcc98208.txt](http://www.fcc.gov/Bureaus/Engineering_Technology/Notices/1998/fcc98208.txt)
- [17] B. Wild and K. Ramchandran, "Detecting primary receivers for cognitive radio applications," in *IEEE DySPAN 2005*, Baltimore, MD, Nov.8–11 2005.
- [18] FCC, "FCC 03-322," Dec. 2003. [Online]. Available: [http://hraunfoss.fcc.gov/edocs\\_public/attachmatch/FCC-03-322A1.pdf](http://hraunfoss.fcc.gov/edocs_public/attachmatch/FCC-03-322A1.pdf)
- [19] M. McHenry, "The Probe Spectrum Access Method," in *IEEE DySPAN 2005*, Baltimore, MD, Nov.8–11 2005, pp. 346–351.
- [20] M. Oliveri, G. Barnett, A. Lackpur, A. Davis, and O. Ngo, "A Scalable Dynamic Spectrum Allocation System with Interference Mitigation for Teams of Spectrally Agile Software Defined Radios," in *IEEE DySPAN 2005*, Baltimore, MD, Nov.8–11 2005, pp. 170–179.

- [21] N. Devroye, P. Mitran, and V. Tarokh, "Achievable rates in cognitive radio," *IEEE Trans. Inform. Theory*, Submitted 2004.
- [22] ———, "Cognitive multiple access networks," *IEEE Trans. Inform. Theory*, Submitted 2005.
- [23] FCC, "FCC 04-113," May 2004. [Online]. Available: [http://hraunfoss.fcc.gov/edocs\\_public/attachmatch/FCC-04-113A1.pdf](http://hraunfoss.fcc.gov/edocs_public/attachmatch/FCC-04-113A1.pdf)
- [24] A. Sahai, N. Hoven, and R. Tandra, "Some fundamental limits on cognitive radio," in *Forty-second Allerton Conference on Communication, Control, and Computing*, Monticello, IL, Oct. 2004.
- [25] R. Tandra, "Fundamental limits on detection in low SNR," Master's thesis, University of California, Berkeley, 2005.
- [26] H. Urkowitz, "Energy detection of unknown deterministic signals," *Proc. IEEE*, vol. 55, pp. 523–531, Apr. 1967.
- [27] N. A. Robert Price, "Detection theory," *IEEE Trans. Inform. Theory*, vol. 7, pp. 135–139, July 1961.
- [28] P. M. F. A. Sonnenschein, "Radiometric detection of spread-spectrum signals in noise of uncertain power," *IEEE Trans. Aerosp. Electron. Syst.*, vol. 28, pp. 654–660, July 1992.
- [29] D. Tse and P. Viswanath, *Fundamentals of Wireless Communication*. New York: Cambridge University Press, 2005.
- [30] W. Gardner, "Signal interception: A unifying theoretical framework for feature detection," *IEEE Trans. Commun.*, vol. 36, pp. 897–906, Aug. 1988.
- [31] ———, "Signal interception: Performance advantages of cyclic-feature detectors," *IEEE Trans. Commun.*, vol. 40, pp. 149–159, Jan. 1992.
- [32] R. G. Gallager, "Residual noise after interference cancellation on fading multipath channels," 1996, appears in the Proceedings of the International Conference on Communications, Computing, Control, and Signal Processing in honor of T. Kailath, Stanford CA, June 1995.
- [33] J. A. Fuemmeler, N. H. Vaidya, and V. V. Veeravalli, "Selecting transmit powers and carrier sense thresholds for CSMA protocols," University of Illinois at Urbana-Champaign, IL, Tech. Rep., Oct. 2004.
- [34] FCC. (2005) KRON-TV at san francisco. [Online]. Available: <http://www.fcc.gov/fcc-bin/tvq?list=0&facid=65526>
- [35] ———. (2005) KRON-TV service contour map. [Online]. Available: <http://www.fcc.gov/fcc-bin/FMTV-service-area?x=TV282182.html>
- [36] M. Franceschetti, J. Bruck, and L. J. Schulman, "A random walk model of wave propagation," *IEEE Trans. Antennas Propagat.*, vol. 52, pp. 1304–1317, May 2004.
- [37] N. Hoven and A. Sahai, "Power scaling for cognitive radio," in *Proc. of the WirelessCom 05 Symposium on Signal Processing*, Maui, HI, June 13–16 2005.
- [38] N. Hoven, "On the feasibility of cognitive radio," Master's thesis, University of California, Berkeley, 2005.
- [39] R. Tandra and A. Sahai, "Fundamental limits on detection in low SNR under noise uncertainty," in *Proc. of the WirelessCom 05 Symposium on Signal Processing*, Maui, HI, June 13–16 2005.
- [40] S. M. Mishra, A. Sahai, and R. W. Broderson, "Cooperative sensing among cognitive radios," in *ICC 2005*, Istanbul, Turkey, June 11–15, 2006.
- [41] V. Paxson and S. Floyd, "Wide area traffic: The failure of poisson modeling," *IEEE/ACM Trans. Networking*, vol. 3, pp. 226–244, June 1998.
- [42] C. Weck, "Validate Field Trials of Digital Terrestrial Television (dvb-t)," Institut fr Rundfunktechnik GmbH Rundfunksystementwicklung Mnchen, Germany, Tech. Rep. [Online]. Available: <http://www.broadcastpapers.com/tvtran/BSDValidateDVBT01.htm>
- [43] M. Gudmundson, "Correlation model for Shadow fading in Mobile Radio Systems," *Electronic Letters*, vol. 27, no. 23, pp. 2145–2146, 1991.
- [44] D. Cabric, S. M. Mishra, and R. W. Brodersen, "Implementation Issues in Spectrum Sensing for cognitive radios," in *Asilomar Conference on Signals, Systems, and Computers*, 2004.

- [45] “Irregular Terrain Model (ITM) (Longley-Rice),” U.S. Department of Commerce NTIA, Tech. Rep. [Online]. Available: <http://flattop.its.bldrdoc.gov/itm.html>
- [46] E. Vistotsky, S. Kuffner, and R. Peterson, “On Collaborative Detection of TV Transmissions in Support of Dynamic Spectrum Sharing,” in *IEEE DySPAN 2005*, Baltimore, MD, Nov.8–11 2005.